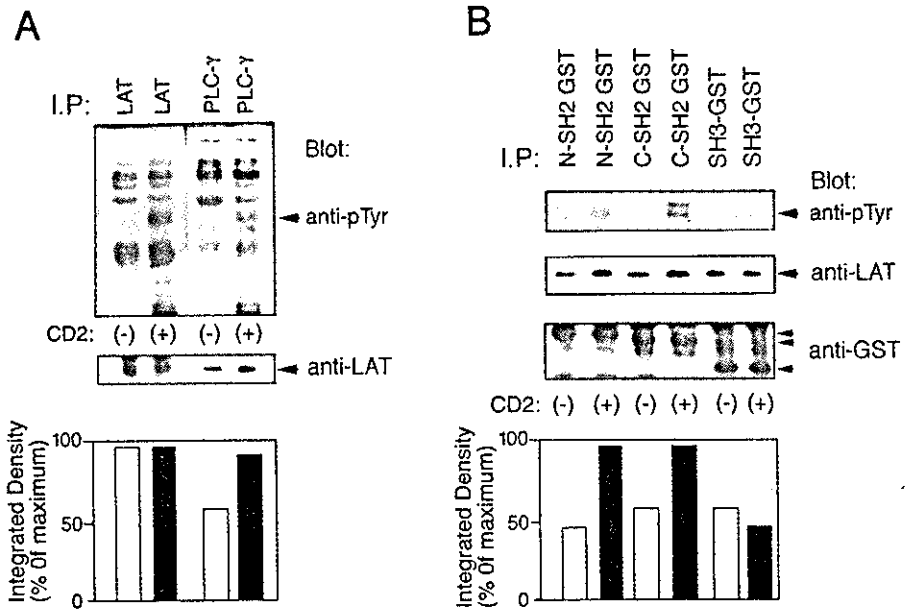

Fig. 6. Interaction between LAT and PLC-γ1 following CD2 stimulation. (A) Association of LAT with PLC-γ1. NK3.3 cells were stimulated by CD2 cross-linking and immunoprecipitated with anti-LAT and anti-PLC-γ1 Ab. Tyrosine phosphorylation and association of LAT with PLC-γ1 were detected by immunoblot. (B) Association of LAT with PLC-γ1 analyzed by an *in vitro* binding assay. After stimulation, lysates were incubated with N-terminal and C-terminal SH2-, or SH3-GST fusion proteins of PLC-γ1 for 2 h at 4°C. Interacting complexes were immunoprecipitated with anti-GST mAb. Quantification of LAT association was performed densitometrically using NIH image software. The peak heights of each density are depicted as percent of maximum value.

mes (a family of granule-associated serine esterases) [36]. After treatment with MβCD, NK3.3 cells were stimulated by CD2 cross-linking for 4 h, and supernatants were assayed for esterase activity using N^{α}-benzyloxycarbonyl-L-lysine thiobenzyl ester (BLTE) as a substrate. We found that MβCD dramatically inhibited granule exocytosis from CD2-activated NK cells in a dose-dependent manner (Fig. 8B).

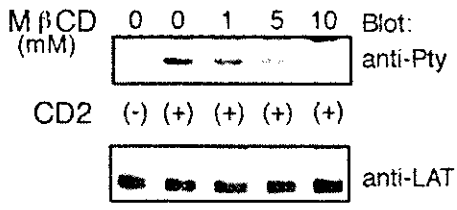

Fig. 7. Effects of MβCD on LAT tyrosine phosphorylation. NK3.3 cells were pretreated with the indicated concentration of MβCD at 37°C for 20 min. Cells were treated with CD2 mAb and stimulated using polybeads coupled to rabbit anti-mouse IgG Ab at 37°C. Detergent-soluble proteins were immunoprecipitated with anti-LAT Ab. The membrane was immunoblotted with anti-pTyr mAb, and then stripped and immunoblotted with LAT Ab.

3 Discussion

Several putative activation receptors, such as CD2, CD16, NKR-P1, 2B4 and chemokine receptors, have been proposed to be involved in NK cell recognition of target cells [2–5, 37]. When an NK cell encounters a target cell, there is an initial activation by triggering receptors that leads to Ca^{2+} mobilization and activation of various kinases. These kinases activate a series of signaling events, ultimately resulting in a polarized secretion of cytotoxic granules. Triggering receptors accumulate in the area of cell-cell contact, creating an immunological synapse. Recently, rafts have been implicated in the organization of the T cell immunological synapse and many of the cytoplasmic proteins involved in T cell activation have been shown to be either raft-resident proteins or selectively recruited to rafts during T cell activation [11, 12]. Thus, lipid rafts may mediate signal transduction by serving as scaffolds to sequester signaling complexes. However, little is known about events leading to the formation of immune synapse and its linkage to activation signals in NK cells.

Yashiro-Ohtani et al. [23] and Yang et al. [24] have reported that CD2 localized in raft fractions in mouse and

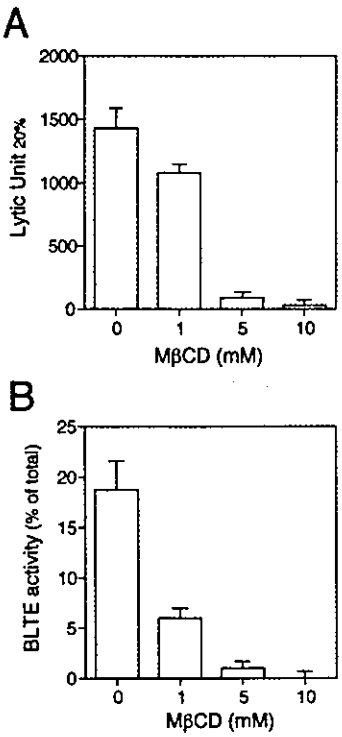

Fig. 8. Effects of MβCD on NK cell functions. NK3.3 cells were pretreated with the indicated concentration of MβCD at 37°C for 20 min before the assay. (A) NK3.3 cytotoxicity against K562 target cells. NK3.3 cells were incubated with calcein-AM labeled K562 cells at titrated effector: target ratios for 4 h at 37°C. After incubation, fluorescence in supernatants was measured and data were expressed as lytic units$_{20\%}$ in 10^7 effector cells. (B) Granule exocytosis from NK 3.3 cells. Cells were stimulated with CD2 mAb-bound polybeads at a ratio of 1:4 for 4 h at 37°C, and supernatants were harvested from each well for BLTE assay. Optical density was read at 405 nm on an ELISA microplate, and the percentage of BLTE activity was calculated.

human T cells, respectively. However, CD2 localization in lipid rafts and the molecular mechanisms that link to intracellular signaling for NK cell activation are still to be elucidated. We have now clearly demonstrated that CD2 cross-linking induced copolarization of rafts and CD2 (Fig. 1), and that a significant amount of CD2 localized in raft fractions of NK3.3 cells (Fig. 3). Using a more physiological system in which NK cells are activated by direct contact with NK-sensitive target, K562 cells, we also observed copolarization of CD2 and rafts at the contact site (Fig. 2). These data suggest that lipid rafts transport NK-activating receptors to the immunological synapse during NK cell cytolytic process. Interestingly, it has been reported that the inhibitory NK immune synapse, transducing negative signals, prevent lipid raft polarization and NK cell cytotoxicity [6–8]. Thus, it is likely that the ability of NK cells to kill target cells is determined by both activating and inhibitory signals through formation of immunological NK synapses.

Although the cytoplasmic domain of CD2 lacks intrinsic kinase activity, CD2 has been reported to be physically associated with *Lck* [38]. Since lipid rafts serve as platforms for GPI-anchored proteins, some transmembrane proteins, cell surface receptors and doubly acylated protein tyrosine kinases of the *src* family [22], this interaction may be explained by our data that CD2 localizes in lipid rafts (Fig. 3). We have previously reported that CD2 cross-linking activates *Syk* tyrosine kinase and transduces signals for NK cell activation [3, 20, 21]. Since it has been reported that signal transduction via CD2 in NK cells is dependent in part on the CD3ζ chain or the γ subunit of FcεR1 expressed in NK cells [39, 40], it is likely that CD2 signaling in NK cells utilizes an analogous cascade to that observed in TCR signaling, *i.e.* CD2 activates *Lck* and *Syk*, and phosphorylates immunoreceptor tyrosine-based activation motifs (ITAM) of the CD3ζ chain, the γ subunit of FcεR1 or the novel transmembrane adapter protein, DAP12 [41], resulting in tyrosine phosphorylation of LAT.

Several lines of evidence demonstrate that tyrosine-phosphorylated LAT recruits critical signaling molecules, including PLC-γ1, Grb2 and PI 3-K as well as Sos and SLP-Vav complex, suggesting that LAT is important in linking the activation of *Syk/ZAP-70* to a number of downstream pathways [13, 16, 17, 37, 42]. Activation of PLC-γ1 results in hydrolyzing phosphatidylinositol 4,5-bisphosphate, which, in turn, increases intracellular free Ca^{2+} concentrations and protein kinase C activity, resulting in enhanced cytoplasmic granule exocytosis [1, 43]. PI 3-K is another important signaling molecule in a variety of cellular process including reorganization of the actin cytoskeleton, induction of cellular survival and protection from apoptosis, antigen- and IL-2 growth factor-mediated activation, membrane ruffling and granule exocytosis [3, 29–31]. In NK cells, Jevremovic et al. have reported that FcγRIII stimulation induced tyrosine phosphorylation and association of LAT with PLC-γ1 [44], which is consistent with our results of CD2-stimulated NK cells (Fig. 6). We previously have reported that CD2 cross-linking induces tyrosine phosphorylation and interaction of cellular proteins with PI 3-K, resulting in NK cell activation [3]. In this paper, data are presented to clearly show that tyrosine-phosphorylated LAT associates with PI 3-K following CD2 stimulation in NK3.3 cells (Fig. 5). These results strongly suggest that LAT may contribute to the recruitment of PI 3-K and PLC-γ1 to the activation sites and that LAT is deeply involved in NK cell activation signaling. It has also been reported that the negative signals through KIR, containing two immunoreceptor

tyrosine-based inhibition motifs (ITIM), recruit SHP-1 and SHP-2, cytoplasmic tyrosine phosphatases. The membrane-proximal ITIM recruits SHP-1 and is itself sufficient to inhibit NK cell killing. The membrane-distal ITIM acts in concert with the proximal ITIM to recruit SHP-2, which then amplifies the signal from SHP-1. SHP-1 and SHP-2 activation leads to the propagation of a downstream signaling cascade that inactivates signaling molecules involved in NK cell activation [45]. Thus, NK cell cytotoxicity is determined by a balance of positive and negative signals, and lipid rafts may serve as scaffolds to regulate NK cell functions.

It has been reported that extraction of raft cholesterol from plasma membrane by MβCD redistributed raft components, and reduced Ca^{2+} responses and tyrosine phosphorylation, inhibited association of the TCR with the cytoskeleton [34, 35]. We observed that treatment of NK cells with MβCD inhibited tyrosine phosphorylation of LAT in a dose-dependent manner (Fig. 7) and that MβCD dramatically reduced NK cell cytolytic activity against target cells and CD2-mediated granule exocytosis from NK cells (Fig. 8A, B). Since the associations of LAT with PI 3-K and PLC-γ1 are dependent on LAT tyrosine phosphorylation (Fig. 5 and 6, respectively), disruption of rafts may inhibit NK cell activities through reducing tyrosine phosphorylation of LAT.

In conclusion, we show that CD2 and rafts copolarized to the sites of NK cell activation and that cross-linking of CD2 induces strong tyrosine phosphorylation of raft-resident LAT, resulting in increased association with PI 3-K and PLC-γ1. Moreover, disruption of lipid rafts by cholesterol depletion markedly reduced LAT tyrosine phosphorylation and NK cell functions, including cytotoxicity and granule exocytosis. These results support the conclusion that raft polarization, resulting in formation of complexes of LAT with PI 3-K and PLC-γ1, are critical events during the development of NK cell-mediated cytotoxicity.

4 Materials and methods

4.1 Cells and cell culture

The human NK cell line, NK3.3, was provided by Dr. Jacki Kornbluth (University of Arkansas Med. Science) and maintained in RPMI 1640 medium supplemented with 10% heat inactivated FCS (Upstate Biotechnology, Inc.: UBI, Lake Placid, NY), 2 mM L-glutamine, penicillin, and 2 nM recombinant IL-2 (Shionogi Co., Ltd., Japan). K562 cells were kindly provided by Dr. M. Maeda (Kyoto University) and maintained in RPMI 1640 medium supplemented with 10% FCS, 2 mM L-glutamine, and penicillin.

4.2 Ab and reagents

mAb against CD11a (LFA-1α: TS1/22; IgG1), CD18 (LFA-1β: TS1/18; IgG1) and CD2 (TS2/18; IgG1) were purified as described previously [46]. $F(ab')_2$ fragment of CD2 mAb was prepared by pepsin digestion and purified by sequential protein A column using Preparation Kit (Pierce, Rockford, IL). Anti-pTyr mAb (4G10), Ab against p85 subunit of PI 3-K and PLC-γ1 were purchased from UBI (Lake Placid, NY). Anti-FcγRIII (CD16: B-E16; IgG1) mAb and PE-conjugated anti-CD2 and anti-CD58 mAb were purchased from Serotec (Oxford, GB) and Becton Dickinson (San Jose, CA), respectively. FITC-conjugated cholera toxin B (CTx), methyl-β-cyclodextrin (MβCD) and control mouse IgG1 (MOPC-31c) were purchased from Sigma-Aldrich (St. Louis, MO). Rabbit antiserum to LAT was kindly provided by Dr. L.E. Samelson (NCI/NIH) [13]. Rabbit anti-mouse IgG mAb and anti-GST mAb were purchased from Cappel (Durham, NC) and Santa Cruz Biotechnology (Santa Cruz, CA), respectively. The ECL immunodetection system and horseradish peroxidase-conjugated goat anti-mouse or anti-rabbit IgG mAb were obtained from Amersham International (Amersham, GB). Polybeads polystyrene microspheres (2.5% solid-latex, diameter = 6 micron, no. 07312) were purchased from Polysciences, Inc. (Warrington, PA).

4.3 Laser scanning confocal microscopy

NK3.3 cells were first stained with FITC-conjugated CTx for 30 min on ice, washed twice in ice-cold PBS containing 0.2% BSA (PBS/BSA), and then incubated with PE-conjugated CD2 mAb for 30 min on ice. After washing in PBS/BSA, cells were resuspended at a final concentration of 10^7 cells/ml in 100 μl RPMI 1640 containing 2% FCS and stimulated with rabbit anti-mouse IgG- or normal rabbit serum (NRS)-bound polybeads at a ratio of 1:2 for 30 min at 37°C in polypropylene round-bottom tubes, in a final volume of 200 μl/tube. After stimulation, cells were cooled with 1 ml ice-cold PBS/BSA containing 0.1% sodium azide, then gently resuspended and placed on glass slides and fixed with 2% paraformaldehyde in PBS. The slides were mounted with coverslips using glycerol/PBS, and examined on an Olympus LSM-GB200 (Olympus, Tokyo, Japan) with an oil immersion lens. Appropriate excitation and barrier filters were used to observe fluorescence.

For assaying conjugation between effector and target cells, NK3.3 cells were stained with FITC-CTx and PE-CD2 mAb. After washing, NK3.3 cells were mixed with K562 cells at a ratio of 1:1, briefly pelleted, and then incubated for 5 min at 37°C. In some experiments, NK3.3 cells labeled with FITC-CTx were mixed with K562 cells labeled with PE-CD58 mAb. Approximately 50 conjugates were evaluated per slide. Photographs of cells shown in figures represent the majority of cells displaying cell-surface staining patterns observed in these experiments.

4.4 Cell stimulation, solubilization and immunoprecipitation

Polybeads were prepared as described elsewhere [47], using 20 μg/ml rabbit anti-mouse IgG, followed by storage with the mAb, and extensive washing prior to use. NK3.3 cells (10^7) were incubated with the indicated Ab for 30 min on ice. After washing, cells were stimulated with rabbit anti-mouse IgG-bound polybeads at a ratio of 1:2 for 30 min at 37°C. Cells were solubilized with Brij lysis buffer containing 50 mM Tris-HCl, pH 7.6, 1% Brij 96, 300 mM NaCl, 5 mM EDTA, 10 μg/ml leupeptin, 10 μg/ml aprotinin, 1 mM phenylmethylsulfonyl fluoride (PMSF) and 1 mM sodium orthovanadate by gentle rocking for 30 min at 4°C. Insoluble material was removed by centrifugation and the supernatants were subjected to immunoprecipitation with Protein G beads precoated with Ab as indicated. For treatment with calf intestine alkaline phosphatase (CIP), immunoprecipitates were incubated with 10 units of CIP (Boehringer) in 40 μl CIP reaction buffer for 1 h.

4.5 GST fusion protein experiments

GST fusion proteins of PI 3-K, p85 C-terminal SH2 (624–718) and N-terminal SH2 (333–428) were purchased from UBI. GST fusion proteins of PLC-γ1 N-terminal SH2 (548–659), C-terminal SH2 (663–760), and SH3 (790–850) were purchased from Santa Cruz Biotechnology. For *in vitro* binding assays using GST fusion proteins, NK3.3 lysates were incubated with the various GST fusion proteins (each 2 μg) in 500 μl of lysis buffer for 2 h at 4°C. Interacting complexes were immunoprecipitated by anti-GST Ab (Santa Cruz) preadsorbed to Protein G beads [20, 21].

4.6 Isolation of a raft fraction in equilibrium density gradients

Raft fractions were prepared as described by Rodgers and Rose [25] with minor modifications [26]. Cells (10^8) were washed with PBS containing 1 mM sodium orthovanadate and 5 mM EDTA, and lysed with 1 ml MS-buffered saline (MBS; 25 mM MES, pH 6.5/150 mM NaCl) containing 1% Triton X-100, 10 μg/ml aprotinin, 10 μg/ml leupeptin, 1 mM PMSF, 1 mM sodium orthovanadate and 5 mM EDTA. The lysate was homogenized with 20 strokes of a Dounce homogenizer, gently mixed with an equal volume of 80% sucrose (w/v) in MBS and placed in the bottom of a 14×95 mm clear centrifuge tube (344060; Beckman, Palo Alto, CA). The sample was then overlaid with 6.5 ml of 30% sucrose and 3.5 ml of 5% sucrose in MBS, and centrifuged at 200,000×g in a Beckman SW40Ti rotor at 4°C for 16 h. Following centrifugation, 12 fractions of 1 ml (excluding the pellet) were collected from the top of the gradient. A half of each gradient fraction was diluted with 10% digitonin in MBS at a final concentration of digitonin to 1%, precleared with protein A-Sepharose (Pharmacia, Piscataway, NJ). To examine the presence of cell surface and intracellular proteins in the density gradient fractions, 16 μl of each fraction was solubilized in 5× sample buffer and electrophoresed.

4.7 Electrophoresis, Western blotting and Immunoblotting

Immunoprecipitated proteins were eluted by boiling in SDS-containing sample buffer and fractionated by SDS-PAGE (8–12% polyacrylamide gels) [48]. Proteins were electrophoretically transferred to polyvinylidene difluoride (PVDF; Immobilon-P) membranes (Sigma). Membranes were incubated for 3 h with either anti-pTyr mAb or Ab as indicated, in PBS containing 0.05% Tween-20 and 10% Blockace (Dainippon Pharm. Co., Japan). Peroxidase-conjugated secondary Ab (Amersham) were used at a 1:1,000 dilution and immunoreactive bands were visualized using ECL (Amersham). In some experiments, densitometry of the protein bands was performed using NIH Image software and the peak heights of each density are depicted as percent of maximum value.

4.8 Cytotoxicity assay and BLTE assay

NK cells were pre-treated with the indicated concentration of MβCD for 20 min at 37°C before the assay. For cytotoxicity assays, target cells (K562) were labeled with calcein-AM (Molecular probes, Leiden, Netherlands) for 30 min at 37°C. Then target cells (5000 per well) and NK3.3 cells were plated into 96-well plates at titrated effector: target (E/T) ratios ranging from 4:1 to 256:1, and incubated for 4 h at 37°C in a humidified atmosphere containing 5% CO_2. After incubation, supernatants were transferred to new wells and fluorescence was measured using a Wallac 1420 ARVO fluoroscan. Assays were performed in triplicate and data were expressed as lytic $units_{20\%}$ in 10^7 effector cells (1 lytic unit containing that number of effector cells lysing 20 % of the target) [49].

For the BLTE assay, IL-2-cultured NK cells were suspended at 10^6 cells/ml in phenol red-free RPMI 1640 (IBL, Fujioka, Japan) containing 0.5% FCS, and 100 μl of aliquots were added to round-bottom microplate wells. Cells were stimulated with CD2 mAb-bound polybeads at a ratio of 1:4 (final volume of 200 μl) for 4 h at 37°C. Wells were incubated at 37°C for 4 h, and 100 μl aliquots were harvested from each well for BLTE assay. The BLTE assay was adapted to 200 μl for use in 96-well as described previously [3, 46]. Optical density was read at 405 nm on an ELISA microplate reader (Iwaki, Osaka, Japan), and the percentage of BLTE activity was calculated.

Acknowledgements: We thank Dr. L. E. Samelson (NCI/NIH) for providing anti-LAT Ab. We also thank Dr. A. Yamauchi (Kagawa University) for his input, and Ms. N. Tani-

mura (Osaka University) for technical help. This work was supported by Grants 11470464, 13557160 and 13226124 form Japanese Ministry of Education, Science and Culture (to H.U.) and the Science Research Promotion Fund of the Japan Private School Promotion Foundation (to N.D.), and the Osaka Dental University Research Foundation (to H.U. and N.D.)

References

1 **Podack, E. R.,** Functional significance of two cytolytic pathways of cytotoxic T lymphocytes. *J. Leukoc. Biol.* 1995. **57:** 548–552.

2 **Storkus, W. J. and Dawson, J. R.,** Target structures involved in natural killing (NK): Characteristics, distribution, and candidate molecules. *Crit. Rev. Immunol.* 1991. **10:** 393–416.

3 **Umehara, H., Huang, J.-Y., Kono, T., Tabassam, F. H., Okazaki, T., Bloom, E. T. and Domae, N.,** Involvement of protein tyrosine kinase p72syk and phosphatidylinositol 3-kinase in CD2-mediated granular exocytosis in natural killer cell line. *J. Immunol.* 1997. **159:** 1200–1207.

4 **Maghazachi, A. A. and Al-Aoukaty, A.,** Chemokines activate natural killer cells through heterotrimeric G-proteins: implications for the treatment of AIDS and cancer. *FASEB J.* 1998. **12:** 913–924.

5 **Yoneda, O., Imai, T., Gouda, S., Inoue, H., Yamauchi, A., Okazaki, T., Yoshie, O., Domae, N. and Umehara, H.,** NK cell-mediated vascular injury. *J. Immunol.* 2000. **164:** 4055–4062.

6 **Lou, Z., Jevremovic, D., Billadeau, D. and Leibson, P. J.,** A balance between positive and negative signals in cytotoxic lymphocytes regulates the polarization of lipid rafts during the development of cell-mediated killing. *J. Exp. Med.* 2000. **191:** 347–354.

7 **Eriksson, M., Ryan, J. C., Nakamura, M. C. and Sentman, C. L.,** Ly49A inhibitory receptors redistribute on natural killer cells during target cell interaction. *Immunology* 1999. **97:** 341–347.

8 **Fassett, M. S., Davis, D. M., Valter, M. M., Cohen, G. B. and Strominger, J. L.,** Signaling at the inhibitory natural killer cell immune synapse regulates lipid raft polarization but not class I MHC clustering. *Proc. Natl. Acad. Sci. USA* 2001. **98:** 14547–14552.

9 **Lanier, L. L.,** On guard-activating NK cell receptors. *Nat. Immunol.* 2001. **2:** 23–27.

10 **Umehara, H., Bloom, E. T., Okazaki, T., Domae, N. and Imai, T.,** Fractalkine and vascular injury. *Trends Immunol.* 2001. **22:** 602–607.

11 **Ilangumaran, S., He, H.-T. and Hoessli, D. C.,** Microdomains in lymphocyte signaling: beyond GPI-anchored proteins. *Immunol. Today* 2000. **21:** 2–7.

12 **Brown, D. A. and London, E.,** Functions of lipid rafts in biological membranes. *Annu. Rev. Cell Dev. Biol.* 1998. **14:** 111–136.

13 **Zhang, W., Sloan-Lancaster, J., Kitchen, J., Trible, R. P. and Samelson, L. E.,** LAT: The ZAP-70 tyrosine kinase substrate that links T cell receptor to cellular activation. *Cell* 1998. **92:** 83–92.

14 **Zhang, W., Trible, R. P. and Samelson, L. E.,** LAT palmitoylation: its essential role in membrane microdomain targeting and tyrosine phosphorylation during T cell activation. *Immunity* 1998. **9:** 239–246.

15 **Tomlinson, M. G., Lin, J. and Weiss, A.,** Lymphocytes with a complex: adapter proteins in antigen receptor signaling. *Immunol. Today* 2000. **21:** 584–591.

16 **Rudd, C. E.,** Adaptors and molecular scaffolds in immune cell signaling. *Cell* 1999. **96:** 5–8.

17 **van Leeuwen, J. E. M. and Samelson, L. E.,** T cell antigen-receptor signal transduction. *Curr. Opin. Immunol.* 1999. **11:** 242–248.

18 **Chan, A. C., Desai, D. M. and Weiss, A.,** The role of protein tyrosine kinases and protein tyrosine phosphatases in T cell antigen receptor signal transduction. *Annu. Rev. Immunol.* 1994. **12:** 555–592.

19 **Davis, S. J. and van der Merwe, P. A.,** The structure and ligand interactions of CD2: implications for T cell function. *Immunol. Today* 1996. **17:** 177–186.

20 **Huang, J., Umehara, H., Inoue, H., Tabassam, F., Okazaki, T., Kono, T., Minami, Y., Tanaka, Y. and Domae, N.,** Differential interaction of Cbl with Grb2 and Crk in CD2-mediated NK cell activation. *Mol. Immunol.* 2000. **37:** 1057–1065.

21 **Umehara, H., Inoue, H., Huang, J.-Y., Kono, T., Minami, Y., Tanaka, Y., Okazaki, T., Bloom, E. T. and Domae, N.,** Role for adapter proteins in costimulatory signals of CD2 and IL-2 on NK cell activation. *Mol. Immunol.* 2002. **38:** 587–596.

22 **Horejsi, V., Drbal, K., Cebecauet, M., Cerny, J., Brdicka, T., Angelisova, P. and Stockinger, H.,** GPI-microdomains: a role in signaling via immunoreceptors. *Immunol. Today* 1999. **20:** 356–361.

23 **Yashiro-Ohtani, Y., Zhou, X.-Y., Ytoyo-Ok, K., Tai, X.-G., Park, C.-S., Hamaoka, T., Abe, R., Miyake, K. and Fujiwara, H.,** Non-CD28 costimulatory molecules present in T cell rafts induce T cell costimulation by enhancing the association of TCR with rafts. *J. Immunol.* 2000. **164:** 1251–1259.

24 **Yang, H. and Reinherz, E. L.,** Dynamic recruitment of human CD2 into lipid rafts. *J. Biol. Chem.* 2001. **276:** 18775–18785.

25 **Rodgers, W. and Rose, J. K.,** Exclusion of CD45 inhibits activity of p56lck associated with glycolipid-enriched membrane domains. *J. Cell Biol.* 1996. **135:** 1515–1523.

26 **Kosugi, A., Sakakura, J., Yasuda, K., Ogata, M. and Hamaoka, T.,** Involvement of SHP-1 tyrosine phosphatase in TCR-mediated signaling pathways in lipid rafts: Targeting of activated SHP-1 to lipid rafts induces a defective function of LAT and impairs T cell activation after TCR engagement. *Immunity* 2001. **14:** 669–680.

27 **Cerboni, C., Gismondi, A., Palmieri, G., Piccoli, M., Luigi, F. and Santoni, A.,** CD16-mediated activation of phosphatidylinositol-3 kinase (PI-3 K) in human NK cells involves tyrosine phosphorylation of Cbl and its association with Grb2, Shc, pp36 and p85 PI-3 K subunit. *Eur. J. Immunol.* 1998. **28:** 1005–1015.

28 **Galandrini, R., Palmieri, G., Paolini, R., Piccoli, M., Frati, L. and Santoni, A.,** Selective binding of shc-SH2 domain to tyrosine-phosphorylated 1562; but not γ-chain upon CD16 ligation on human NK cells. *J. Immunol.* 1997. **159:** 3767–3773.

29 **Ward, S. G., Reif, K., Ley, S., Fry, M. J., Waterfield, M. D. and Cantrell, D. A.,** Regulation of phosphoinositide kinase in T cells: Evidence that phosphatidylinositol 3-kinase is not a substrate for T cell antigen receptor-regulated tyrosine kinases. *J. Biol. Chem.* 1992. **267:** 23862.

30 **Kanakaraj, P., Duckworth, B., Azzoni, L., Kamoun, M., Cantley, L. C. and Perussia, B.,** Phosphatidylinositol-3 kinase activation induced upon FcγRIIIA-ligand interaction. *J. Exp. Med.* 1994. **179:** 551–558.

31 **Jiang, K., Zhong, B., Gilvary, D. L., Corliss, B. C., Hong-Geller, E., Wei, S. and Djeu, J. Y.,** Pivotal role of phosphoinositide-3 kinase in regulation of cytotoxicity in natural killer cells. *Nat. Immunol.* 2000. **1:** 419–425.

32 **Gibbins, J. M., Briddon, S., Shuters, A., van Vugt, M. J., van de Winkel, J. G. J., Saito, T. and Watson, S. P.,** The p85 subunit of phosphatidylinositol 3-kinase associates with the Fc receptor γ-chain and linker for activator of T cells (LAT) in platelets stimulated by collagen and convulxin. *J. Biol. Chem.* 1998. **273:** 34437–34443.

33 **Simons, K. and Ikonen, E.,** Functional rafts in cell membranes. *Nature* 1997. **387:** 569–572.

34 **Klein, U., Gimpl, G. and Fahrenholz, F.,** Alteration of the myometrial plasma membrane cholesterol content with β-Cyclodextrin modulates the binding affinity of the oxytocin receptor. *Biochemistry* 1995. **34:** 13784–13793.

35 **Xavier, R., Brennan, T., Li, Q., McCormack, C. and Seed, B.,** Membrane compartmentation is required for efficient T cell activation. *Immunity* 1998. **8:** 723–732.

36 **Kagi, D., Ledermann, G., Burki, K., Zinkernagel, R. M. and Hengartner, H.,** Molecular mechanisms of lymphocyte-mediated cytotoxicity and their role in immunological protection and pathogenesis in vivo. *Annu. Rev. Immunol.* 1996. **14:** 207–232.

37 **Bottino, C., Augugliaro, R., Castriconi, R., Nanni, M., Biassoni, R., Moretta, L. and Moretta, A.,** Analysis of the molecular mechanism involved in 2B4-mediated NK cell activation: evidence that human 2B4 is physically and functionally associated with the linker for activation of T cells. *Eur. J. Immunol.* 2000. **30:** 3718–3722.

38 **Bell, G. M., Fargnoli, J., Bolem, J. B., Kish, L. and Imboden, J. B.,** The SH3 domain of p56lck binds to proline-rich sequences in the cytoplasmic domain of CD2. *J. Exp. Med.* 1996. **183:** 169–178.

39 **Spruyt, L. L., Glennie, M. J., Beyers, A. D. and Williams, A. F.,** Signal transduction by the CD2 antigen in T cells and natural killer cells: Requirement for expression of a functional T cell receptor or binding of antibody Fc to the Fc receptor, FcγRIIIA (CD16). *J. Exp. Med.* 1991. **174:** 1407–1415.

40 **Moingeon, P., Lucich, J. L., McConkey, D. J., Letourneur, F., Malissen, B., Kochan, J., Chand, H.-C., Rodewald, H.-R. and Reinherz, E. L.,** CD31562; dependence of the CD2 pathway of activation in T lymphocytes and natural killer cells. *Proc. Natl. Acad. Sci. USA* 1992. **89:** 1492–1496.

41 **Lanier, L. L. and Bakker, A. B. H.,** The ITAM-bearing transmembrane adaptor DAP12 in lymphoid and myeloid cell function. *Immunol. Today* 2000. **21:** 611–614.

42 **Finco, T. S., Kadlecek, T., Zhang, W., Samelson, L. E. and Weiss, A.,** LAT is required for TCR-mediated activation of PLCγ1 and the Ras pathway. *Immunity* 1998. **9:** 617–626.

43 **Henkart, P. A., Williams, M. S. and Nakajima, H.,** Degranulating cytotoxic lymphocytes inflict multiple damage pathway on target cells. *Curr. Top. Microbiol. Immunol.* 1995. **198:** 75–93.

44 **Jevremovic, D., Billadeau, D. D., Schoon, R. A., Dick, C. J., Irvin, B. J., Zhang, W., Samelson, L. E., Abraham, R. T. and Leibson, P. J.,** A role for the adapter protein LAT in human NK cell-mediated cytotoxicity. *J. Immunol.* 1999. 2453–2456.

45 **Bruhns, P., Marchetti, P., Fridman, W. H., Vivier, E. and Daeron, M.,** Differential roles of N- and C-terminal immunoreceptor tyrosine-based inhibition motifs during inhibition of cell activation by killer cell inhibitory receptors. *J. Immunol.* 1999. **162:** 3168–3175.

46 **Umehara, H., Takashima, A., Minami, Y. and Bloom, E. T.,** Signal transduction via phosphorylated adhesion molecule, LFA-1β (CD18), is increased by culture of natural killer cells with IL-2 in the generation of lymphokine-activated killer cells. *Int. Immunol.* 1993. **5:** 19–27.

47 **Umehara, H., Huang, J.-Y., Kono, T., Tabassam, F. H., Okazaki, T., Gouda, S., Nagano, Y., Bloom, E. T. and Domae, N.,** Co-stimulation of T cells with CD2 augments TCR-CD3-mediated activation of protein tyrosine kinase p72syk, resulting in increased tyrosine phosphorylation of adapter proteins, Shc and Cbl. *Int. Immunol.* 1998. **10:** 833–845.

48 **Umehara, H., Minami, Y., Domae, N. and Bloom, E. T.,** Increased processing of lymphocyte function-associated antigen-1 in human natural killer cells stimulated with IL-2. *Int. Immunol.* 1994. **6:** 1071–1080.

49 **Bloom, E. T. and Korn, E. L.,** Quantification of natural cytotoxicity by human lymphocyte subpopulations isolated by density: heterogeneity of the effector cells. *J. Immunol. Methods* 1983. **58:** 323–325.

Correspondence: Hisanori Umehara, Department of Rheumatology and Clinical Immunology, Kyoto University Graduate School of Medicine, Shogoin-Kawahara-cho, Sakyo-ku, Kyoto 606-8507, Japan
Fax: +81-75-751-4338
e-mail: umehara@kuhp.kyoto-u.ac.jp

Clin Exp Immunol 2002; 130:224–232

The transmembrane form of TNF-α drives autoantibody production in the absence of CD154: studies using MRL/Mp-*Fas*^{lpr} mice

T. FUJII*†, M. OKADA*‡, T. MIMORI† & J. CRAFT* *Section of Rheumatology, Department of Internal Medicine, Yale School of Medicine, USA, and †Department of Rheumatology and Clinical Immunology, Kyoto University Graduate School of Medicine, Kyoto, Japan

(Accepted for publication 20 July 2002)

SUMMARY

It is generally accepted that the interaction between CD40 and its ligand (CD154) plays a decisive role in contact-dependent help for T and B cells. In CD154-deficient MRL/Mp-*Fas*^{lpr} (MRL/*lpr*) mice, however, high titres of IgG2a-type autoantibodies against small nuclear ribonucleoproteins (snRNPs) are observed. We successfully isolated two CD154-deficient MRL/*lpr* Th1 lines, which could provide B cell help for anti-snRNP antibody production. The proliferative responses of the Th1 cell lines were MHC class II (I-E^k)-restricted. Although syngeneic B cell proliferation was induced by Th1 lines in both a contact-dependent and -independent manner, the soluble form of TNF-α (sTNF-α) was not involved in contact-independent B cell proliferation. On the other hand, both anti-TNF-α and TNF-receptor 2 (TNF-R2, p75) monoclonal antibody (MoAb) blocked contact-dependent B cell proliferation, suggesting that the transmembrane form of TNF-α (mTNF-α)–TNF-R2 co-stimulation participates in B cell activation. Similarly, anti-TNF-α and TNF-R2 MoAb inhibited anti-snRNP antibody production *in vitro*, but anti-CD154 or TNF-R1 MoAb did not. These results indicate that the interaction of mTNF-α on activated Th1 cells with TNF-R2 on B cells may be involved in the autoimmunity seen in MRL mice, and that the blockade of CD40-CD154 co-stimulation may not always be able to suppress some Th1-related manifestations of lupus.

Keywords autoantibodies CD154 co-stimulation lupus TNF-α

INTRODUCTION

Human systemic lupus erythematosus (SLE) is an autoimmune disease characterized by the production of autoantibodies against many nuclear antigens such as chromatin, DNA and certain RNA-associated proteins, including anti-small nuclear ribonucleoproteins (anti-snRNP) antibodies. Several mouse lupus models display autoimmune manifestations reminiscent of SLE, including the MRL/Mp (MRL-+/+) strain that develops a syndrome nearly indistinguishable from the human disease, including marked humoral autoimmunity such as anti-Sm antibody [1]. MRL/Mp-*Fas*^{lpr} (MRL/*lpr*) mice also develop spontaneously a severe disease resembling SLE, especially immune-complex glomerulonephritis, with the generation of IgG autoantibodies to self-antigens such as chromatin, dsDNA, snRNPs and IgG (rheumatoid factors; RF) [2].

A large number of investigations have established that the pathogenesis of MRL lupus mainly requires CD4$^+$ $\alpha\beta$T cells, which help to stimulate autoreactive B cells [3–5]. These studies have demonstrated that a lack of such cells cause substantial reductions in autoantibody production and glomerulonephritis. In addition, CD4$^+$ $\alpha\beta$T cells that help autoantibody production have been isolated from other mouse strains [6,7]. Autoantibodies produced by MRL mice display evidence of Ag selection [8], suggesting that autoreactive CD4$^+$ $\alpha\beta$ T cells drive autoantigen-specific autoantibody production. This notion is supported by the finding that genetic elimination of autoantigen-specific $\alpha\beta$T cells in MRL mice eliminate autoantibody production and end-organ disease [9].

The binding of CD40 ligand (CD154), a type II membrane protein transiently expressed on activated CD4$^+$ T cells [10], to CD40 on B cells plays a critical role in T–B collaboration, including the initiation of immunoglobulin (Ig) synthesis and class

Correspondence: Takao Fujii, Department of Rheumatology and Clinical Immunology, Kyoto University Graduate School of Medicine, 54 Shogoin-Kawahara-cho, Sakyo-ku, Kyoto 606–8507, Japan.

E-mail: takfujii@kuhp.kyoto-u.ac.jp

‡Current address: American Hospital of Paris, Neuilly Cedex, 109–92202, France.

switching in response to thymus-dependent (TD) antigens [11–14], as well as playing a role in the formation of germinal centres and the development of memory B cells [14,15]. In CD154-deficient mice, antigen-specific T cell priming is impaired as a result of the failure to initiate a specific T cell immune response to TD antigens [16]. Along with the apparent requirement for CD4$^+$ $\alpha\beta$ T cells, CD154 appears to be instrumental in IgG autoantibody production and end-organ disease in murine and probably human lupus. Support for this notion comes from the observations that administration of anti-CD154 antibody to autoimmune SNF_1 and (NZB × NZW) F_1 lupus-prone mice inhibits anti-dsDNA synthesis and glomerulonephritis [17,18], and that human subjects with SLE show increased CD154 levels on both T and B cells [19,20].

We previously characterized CD154-deficient lupus-prone MRL/*lpr* mice and found that these animals lacked anti-dsDNA and RF as well as lacking fully developed glomerulonephritis. Surprisingly, however, the CD154-deficient MRL/*lpr* mice underwent Ig class switching to IgG2a with Ig levels much higher than those of control, non-autoimmune mice, and showed partial maintenance of IgG2a anti-snRNP antibody responses [21]. These results indicate that CD40–CD154 co-stimulation is required to provide contact-dependent help for anti-dsDNA antibody production in MRL mice, although IgG class switching and the generation of IgG anti-snRNP antibody do not necessarily rely upon T cell help mediated via CD154 in MRL/*lpr* mice.

The study presented here demonstrates that the autoreactive CD4$^+$ $\alpha\beta$ Th1 cells generated by us have the capacity to provide B cell help for the production of IgG anti-snRNP antibody *in vitro*, and that the transmembrane form of TNF-α (mTNF-α)–TNF receptor (TNF-R) system can be substituted for the CD40–CD154 co-stimulation required for the production of IgG autoantibodies. These observations suggest that mTNF-α expression on activated T cells is involved in lupus autoimmunity and that blockade of CD40–CD154 co-stimulation might be insufficient to suppress some manifestations related to the Th1 response of lupus.

MATERIALS AND METHODS

Mice

MRL/Mp-*Fas^{lpr}* mice (MRL/*lpr* mice, purchased from the Jackson Laboratory, Bar Harbor, ME, USA) were bred with female CD154-deficient 129/SvJ × C57BL/6 (129 × B6 CD154-deficient) mice [13] to produce F_1 offspring heterozygous for *lpr* (mutant *Fas* gene) and for CD154. The animals were then back-crossed to the MRL background to the N8 generation, followed by intercrossing and analysis for wild-type and mutant CD154 and *Fas* by PCR [21]. These mice were bred and housed in specific pathogen-free facilities at the Yale School of Medicine.

Generation of autoreactive T cell lines from CD154-deficient MRL/lpr mice

Autoreactive T cells were isolated and cloned according to Naiki's method [7] with some modifications. A single cell suspension of lymph node cells was prepared from three different 4-month-old, anti-snRNP antibody-positive CD154-deficient MRL/*lpr* mice [21]. The cells were treated with red blood cell lysis buffer (Sigma Chemical Co., St Louis, MO, USA). Initially, 4×10^6/ml of cells were cultured in 24-well tissue culture plates with Click's medium (Irvine Scientific, Santa Ana, CA, USA) supplemented with 10% FCS, antibiotics, L-glutamine and 2-ME. The irradiated (3000 rad) syngeneic APC (2×10^6/ml) were added weekly along with 10 μ/ml mouse rIL-2 (R&D systems, Minneapolis, MN, USA). After 1 month, cells were transferred to 96-well plates at a concentration of five cells/well for limiting dilution. Growing cells were harvested and expanded in 24-well plates for further study. In some experiments, autoreactive Th1 and Th2 cell lines (5-1 and 4-1), which were derived from CD154-intact MRL/*lpr* mice using the same method and not reactive for specific antigens, were used as controls.

Flow cytofluorometric analysis

T cell lines were analysed by flow cytometry using anti-TCR-Cβ (H57-597-FITC), anti-TCR$\gamma\delta$ (GL3-PE), anti-CD4 (H129·19-FITC) and anti-CD8 (53–6·7-PE). For detection of CD154 or mTNF-α, cells after stimulation with plate-bound anti-CD3ε monoclonal antibody (MoAb) (5 μg/ml) were stained with PE-conjugated anti-CD154 (MR1, PharMingen, San Diego, CA, USA) or anti-TNF-α (G281-2626, PharMingen). Stained cells were analysed with a FACScan™ flow cytometer and using CellQuest™ software (Becton Dickinson, Mountain View, CA, USA).

Proliferation assays

For T cell proliferation assays, T cell lines (1×10^5/well) were co-cultured with 5×10^5 irradiated (3000 rad) splenocytes from CD154-deficient MRL/*lpr* mice as APC in triplicate for 3 days in round-bottomed, 96-well microtitre plates. Before the initiation of culture, APC were incubated with either crude ENA (extractable nuclear antigen, 1 mg/ml) prepared from murine Ehrlich ascites cells as described previously [22] or with medium (control) at 37°C for 2 h. [^{3}H]-labelled thymidine (1 μCi, Amersham, Arlington Heights, IL, USA) was added to each well during the last 16 h of culture, and cells were harvested with a semi-automatic cell harvester (Skatron Instruments, Sterling, VA, USA). The incorporated radioactivity was measured with a β-plate scintillation counter (Beckman Instruments, Fullerton, CA, USA).

For B cell proliferation assays, MRL/*lpr* B cells were purified from splenocytes of CD154-deficient MRL/*lpr* mice using Cellect™ Mouse B (Biotex Laboratories Inc., Edmonton, Canada) followed by further T cell depletion using anti-Thy1·2 antibody (HO-13–4) and Low-Tox-M rabbit complement (Accurate Chemical & Scientific Corporation, Westbury, NY, USA). The B cell purity was >95% as determined by flow cytometry. Purified B cells (5×10^4 for 96-well plates and 25×10^4 for 24-well plates) were co-cultured with irradiated (1500 rad) T cell lines (2×10^4 for 96-well plates and 10×10^4 for 24-well plates) for 3 days. One μCi of [^{3}H]-labelled thymidine was added for the last 16 h of culture, cells were harvested and the incorporated radioactivity measured. A membrane insert (0·4 μm pore size, Becton Dickinson Labware, Franklin Lakes, NJ, USA) was used in some experiments to prevent contact between T cell lines and B cells. The separated T and B cells were co-cultured in 24-well culture plates for 48 h, followed by the addition of 4 μCi of [^{3}H]-labelled thymidine. After 16 h, cells above and below the membrane were mixed, and harvested immediately after transfer from 24-well plates to 96-well plates.

For blockade of T or B cell proliferative responses, monoclonal antibodies to I-E^k (14-4-4S, PharMingen, dialysed before use), I-A^k (10–3·6,. PharMingen, dialysed before use), CD154 (MR1, NA/LE, PharMingen), IFN-γ (R4–6A2, NA/LE, PharMingen), IL-2 (Genzyme, Cambridge, MA, USA), TNF-α (G281-2626, NA/LE, PharMingen), TNF-R1 and R2 (p55[55R-170·1]

and p75 [TR75-54·7, a gift from R.D. Schreiber, Washington University School of Medicine]) [23] were used.

In vitro *helper assay*
T cell lines (5×10^5 cells/well) were co-cultured with 2×10^6 purified MRL/*lpr* B cells in 24-well plates for 1 week. Culture supernatants were then harvested, and the concentration of anti-snRNP antibodies determined by ELISA (described below). To determine if antibody production was enhanced via soluble factors (e.g. cytokines), a membrane insert was used to prevent contact between the T cell lines and B cells. Non-autoreactive controls consisted of a T cell line derived from antipigeon cytochrome *c* (PCC) TCR transgenic TCR-α-/-TCRβ-/- MRL/*lpr* mice [9] and purified B cells of PCC-immunized MRL/*lpr* mice.

Determination of anti-snRNP antibodies by ELISA
For detection of anti-snRNP antibody, mouse snRNPs (1 μg/ml) in carbonate buffer, pH 9·6, were coated on Serocluster 'U' Vinyl Plates (Costar, Cambridge, MA, USA) overnight at 4°C. Mouse sera were diluted 1 : 100 with PBS containing 3% BSA and incubated at room temperature for 2 h, followed by detection of bound IgG with alkaline phosphatase-conjugated antimouse IgG (Southern Biotechnology Associates Inc., Birmingham, AL, USA) at $O.D._{405nm}$ in a microtitre ELISA reader. Anti-dsDNA antibodies were measured with Rubin's methods [24].

RESULTS

*Antinuclear antibody production and CD4$^+$ $\alpha\beta$ T cells in CD154-deficient MRL/*lpr *mice*
The levels of anti-dsDNA and -snRNP antibody, as determined by ELISA using purified autoantigens as substrates, were significantly higher in CD154-intact MRL/*lpr* mice than in their CD154-deficient counterparts; however, a number of the latter mice produced comparable amounts of anti-snRNP antibody to those of the CD154-intact animals [21]. The subclass of the higher titre anti-snRNP antibody in CD154-deficient mice was IgG2a, whereas IgG1 and IgG3 anti-snRNP antibody were also detected in CD154-intact mice [21].

The CD44^{high}CD45RB^{high} MRL T cells, which were assured to be effectors, developed in CD154-deficient MRL/*lpr* mice, while CD4$^+$ naive (CD44^{low}CD45RB^{intermed}) $\alpha\beta$ T cells remained in the spleen (unpublished data). The development of memory T cells in these mice, however, was severely impaired because the number was much lower than that in CD154-intact 129 × B6 or MRL/*lpr* of the same age (data not shown).

*T cell lines derived from CD154-deficient MRL/*lpr *mice*
Twenty-six T cell lines were isolated by limiting dilution from three anti-snRNP antibody-positive MRL/*lpr* mice deficient in CD154. Five of these T cell lines were selected for further studies (Table 1) as they expressed both $\alpha\beta$ TCR and CD4 and proliferated in response to crude ENA as a source of snRNPs. These lines all lacked CD154 expression after stimulation with PMA (10 ng/ml) and ionomycin (500 ng/ml)/anti-CD3ϵ MoAb (5 μg/ml). The background stimulation indexes (SI) for proliferation of these Th lines were calculated by averaging their responses to histone, dsDNA or medium. The mean values of background SI + 2 s.d. for these five T cell lines that responded to ENA were 1·49 for C2, 1·42 for G1, 1·33 for G2, 1·52 for P5 and 1·72 for E7. The five lines selected showed increased proliferative responses when co-cultured with syngeneic APC with ENA (Table 1) compared with background levels, strongly suggesting that these lines recognize some self-murine ENA. T cell proliferative responses were MHC class II-restricted, as anti-I-E^k MoAb selectively inhibited the proliferation of four lines (C2, G1, G2, P5). Proliferation of the E7 line also appeared to be I-E^k-restricted, although inhibition was incomplete.

In the presence of irradiated splenocytes from CD154-deficient MRL/*lpr* mice as a source of APC, the lines released either IFN-γ or IL-4 as respective indicators of Th1 or Th2 profiles (data not shown). Four of the five lines (C2, G1, G2, and P5) released IFN-γ after 24 and 72 h incubation, suggesting they had a Th1 phenotype. The last line, E7, released a small amount of IL-4 after 72 h incubation (indicating a Th0 or Th2 phenotype). Additionally, after stimulation with anti-CD3ϵ MoAb, the soluble form of TNF-α (sTNF-α) was detected in the culture supernatant of CD154-deficient Th1 lines (G1 and P5) and the CD154-intact autoreactive Th1 line (5-1), but not the control Th2 line (4-1).

mTNF-α and CD154 expression was examined on autoreactive Th1 or Th2 lines (Fig. 1). CD154 expression was observed on both Th1 and Th2 cells at 12 h, and later continued expression was seen in the Th2 line (4-1). Maximum expression of mTNF-α was observed after 24 h stimulation. mTNF-α but not CD154 expression was observed after 48 h stimulation in the 5-1 and P5 lines (data not shown) indicating that the expression of mTNF-α was predominantly induced on Th1 cells and followed CD154 expression.

Table 1. Autoreactive T cell lines derived from CD154-deficient MRL/*lpr* mice

Isolated T cell lines	T cell proliferation with APC/ENA (SI)[a]	T cell proliferation with APC/ENA[b]			% inhibition (anti-E^k/IgG2a)	TCR Vβ usage
		+ IgG2a	anti-E^k	anti-A^k		
C2	1·52	14 531	3 004	12 964	77	Vβ6
G1	1·74	39 582	3 343	36 788	92	Vβ8·1/8·2
G2	1·36	66 534	3 952	56 638	95	Vβ10
P5	3·45	26 136	4 837	18 765	81	Vβ8·3
E7	3·88	31 249	14 468	33 245	54	Vβ14

[a][^{3}H]-thymidine incorporation (cpm) in the presence of extractantibodyle nuclear antigen (ENA)/[^{3}H]-thymidine incorporation (cpm) in the absence of ENA. [b][^{3}H]-thymidine incorporation (cpm) in the presence of ENA with the antibodies shown. Mean cpm of triplicate culture is given; s.d. within each experiment were <10%.

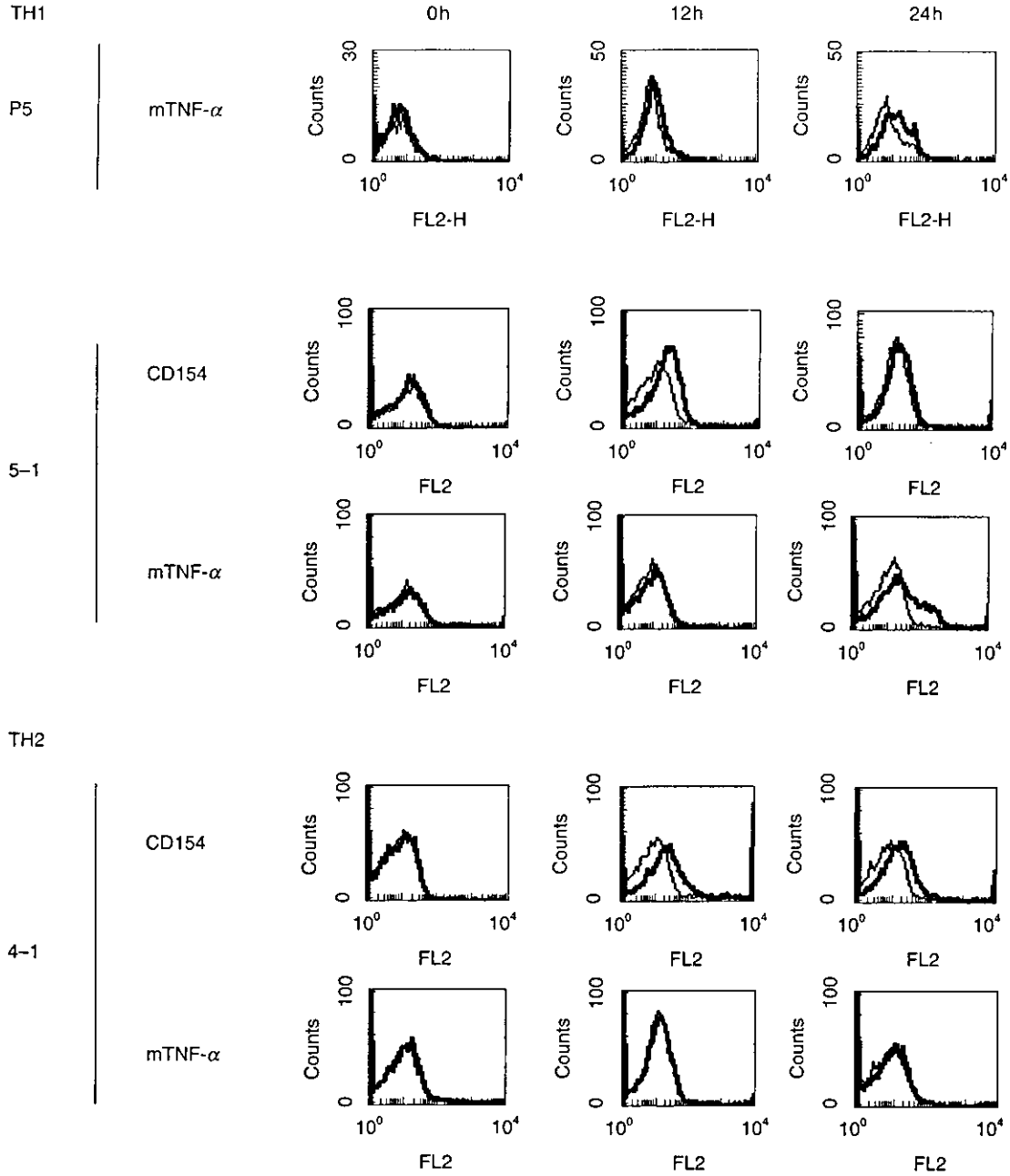

Fig. 1. CD154 and the transmembrane form of TNF-α (mTNF-α) on activated MRL/*lpr* T cell lines. CD154-intact autoreactive Th1 (5-1), and Th2 (4-1) lines and CD154-deficient Th1 (P5) were stimulated with plate-bound anti-CD3ε MoAb (5 μg/ml) for the indicated time. CD154 was not expressed on P5 during 0–48 h stimulation with anti-CD3ε MoAb. Bold lines show staining with anti-CD154 or TNF-α MoAb, and regular lines show isotype control.

CD154-deficient T cell lines promote contact-dependent and -independent B cell proliferation

B7-2 (CD86) expression on MRL B cells was enhanced after co-culture with the CD154-deficient Th1 line (G1) for 24 h and 48 h (data not shown). All the lines induced B cell proliferative responses, which anti-CD154 MoAb (MR1) could not block (see Fig. 2a for a representative result). Anti-CD154 MoAb inhibited the B cell proliferation induced by the CD154-intact Th1 line 5-1, but not that induced by either of the CD154-deficient Th1 lines G1 or P5. To determine if B cell proliferation is contact-dependent, a membrane insert was used to prevent contact by the T cell lines with purified B cells (Fig. 2b). The CD154-deficient line (P5) induced substantial proliferation of B cells either with or without a membrane insert between irradiated P5 and purified B cells, indicating that P5 stimulates a B cell proliferative response in both a contact-dependent and -independent manner. In addition, under the same conditions, anti-IFN-γ or IL-2 MoAb partially inhibited B cell proliferation but anti-TNF-α did not.

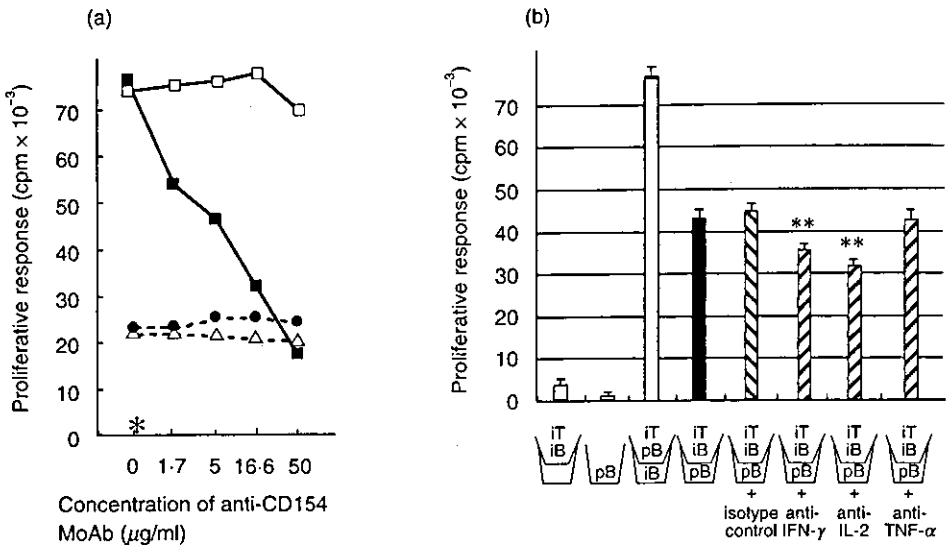

Fig. 2. B cell proliferative responses to autoreactive Th1 lines. (a) Anti-CD154 MoAb (MR1) dramatically inhibited B cell proliferation induced by the CD154-intact line (5-1), but not that by the CD154-deficient line (G1 or P5). (b) A membrane insert (∪) was used to prevent contact by T cell line (P5) with B cells. Irradiated (1500 rad) T cells, which do not proliferate themselves, enhanced purified B cell proliferation. Irradiated (3000 rad) B cells are thought to promote cytokine production from the T cell line as an APC. CD154-deficient lines induce B cell proliferation both in a contact-dependent and -independent manner; however, contact-independent B cell proliferation (black bar) was not inhibited at all by anti-TNF-α MoAb, but was inhibited by anti-IFN-γ or IL-2 MoAb (hatched bar). Concentration of MoAb or isotype control: 25 μg/ml. This figure shows the representative results of three experiments. iT; irradiated T cells (P5), pB; purified B cells, iB; irradiated B cells. $^{**}P < 0.01$ (*versus* isotype control). (a) □, 5-1 (with hamster IgG); ●, G1; △, P5; ■, 5-1; *B cells alone.

These results indicate that contact-independent T cell-mediated B cell proliferation is partially dependent on IFN-γ and IL-2, but not on sTNF-α.

Involvement of mTNF-α and TNF-R in CD154-independent B cell activation

Next, to clarify whether the mTNF-α-TNF-R pathway participates in contact-dependent B cell proliferation, anti-TNF-α or TNF-R MoAb was added to the co-cultures of irradiated lines and purified B cells (Fig. 3). Anti-TNF-α MoAb induced a reduction of about 50% in the B cell proliferative responses induced by a CD154-deficient line (G1 or P5). As sTNF-α was not involved in contact-independent B cell proliferation, this result indicates that the anti-TNF-α MoAb completely abrogates contact-dependent B cell proliferation, and suggests that mTNF-α is responsible for triggering B cell proliferation. Anti-TNF-R2 MoAb also inhibited the proliferative responses induced by both CD154-deficient and intact Th1 lines. Anti-TNF-R1 MoAb inhibited B cell proliferation, but only at a high concentration (= 25 μg/ml).

We next examined whether our CD154-deficient Th1 cell lines had the capacity to provide B cell help for autoantibody production *in vitro* (Fig. 4a). While anti-dsDNA antibody was not released from CD154-deficient B cells after co-cultures with the lines (data not shown) two of the five lines, G1 and P5, induced high levels of SI, especially in the absence of the membrane insert, suggesting that both provide contact-dependent help for anti-snRNP antibody production. With the membrane insert, the SI of CD154-deficient lines was the same as that of PCC-Tg T cells, which is thought to constitute contact-independent help [9]. Moreover, in *in vitro* helper assays, both anti-TNF-α and TNF-R2 MoAb inhibited anti-snRNP antibody production but anti-CD154 and TNF-R1 MoAb did not (Fig. 4b). Anti-IFN-γ MoAb also inhibited anti-snRNP antibody production, indicating that IFN-γ is also involved in autoantibody production in a contact-independent manner.

DISCUSSION

We successfully isolated two autoreactive CD4$^+$ αβ Th1 cell lines from CD154-deficient MRL/*lpr* mice. These lines (G1 and P5) have the capacity to provide B cell help for IgG anti-snRNP antibody production in a contact-dependent manner. Co-stimulation of mTNF-α, which is expressed predominantly on Th1 cells, and TNF-R2 was mainly involved in the production of IgG autoantibodies. In a previous study, we demonstrated that CD154-deficient MRL/*lpr* mice exhibited IgG2a class switching similar to that seen in wild-type MRL/*lpr* mice, and produced anti-snRNP, but not anti-dsDNA antibody [21]. These results indicate that CD154 is required for a high titre of anti-dsDNA antibody production, but that IgG class switching and the genesis of IgG2a anti-snRNP antibody are not necessarily dependent upon the pathway mediated via CD154 in lupus-prone MRL/*lpr* mice.

B cells or MHC class II has a critical role in T cell activation during the generation of systemic autoimmunity [25,26]. The MHC class II molecule (I-E^k) was required for the proliferation and IFN-γ secretion of CD154-deficient MRL Th cells. Superantigens including endogenous Mtvs (from mouse mammary tumour virus), however, do not seem to be involved in the proliferation of our Th1 lines because the proliferation of the G1 and P5 lines was increased in the presence of extractable nuclear antigens. Papiernik *et al.* showed that clonal deletion of Vβ6$^+$ CD4$^+$ T cells by Mtv-6-SAG was avoided in MRL/*lpr* mice [27]. The

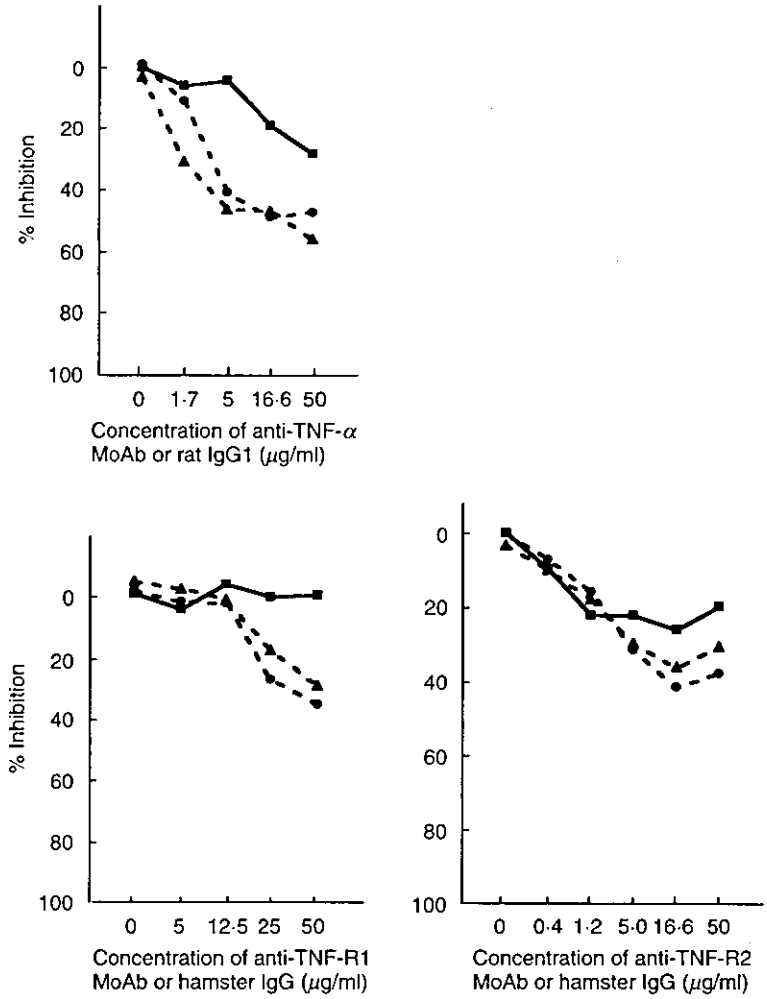

Fig. 3. Inhibition by anti-TNF-α/TNF-R MoAb of B cell proliferative responses to CD154-intact (5-1) or -deficient (G1 and P5) Th1 cell lines. Anti-TNF-α MoAb and anti-TNF-R2 MoAb partially inhibit B cell proliferative responses, and are therefore thought to be mediated via contact-dependent T cell help. Anti-TNF-R1 MoAb also seems to block proliferation by G1 and P5, although a high concentration (>25 μg/ml) was required. Rat IgG1 and hamster IgG constitute isotype controls of anti-TNF-α and anti-TNF-R1 or R2 MoAb, respectively. % Inhibition = (1-{[^{3}H]-thymidine uptake with blocking MoAb (cpm)/[^{3}H]-thymidine uptake with isotype control(cpm)}) × 100. Mean cpm of triplicate cultures was used for calculations; s.d. for each experiment was less than 10%. ■, 5-1; ●, G1; ▲, P5.

influence of known Mtvs on MRL/*lpr* T cell receptor should be determined to exclude involvement of the maternally inherited superantigen-induced T cell response.

On the other hand, the dramatic inhibition by anti-CD154 MoAb of B cell proliferation with the CD154-intact line indicates that CD40-CD154 signalling is profoundly involved in B cell up-regulation even after T cells have been primed [28]. CD154-deficient lines, nevertheless, still induced B7-2 expression, syngeneic B cell proliferation and anti-snRNP secretion, indicating that MRL Th1 cells have the capacity to provide B cell help for autoantibody production in the absence of CD154. The insertion of a membrane to separate Th1 and B cells reduces the B cell proliferation and autoantibody production, suggesting that the Th1 cell lines stimulate B cells both in both a contact-dependent and -independent manner.

mTNF-α is processed to generate sTNF-α by a disintegrin metalloproteinase, known as the TNF-α-converting enzyme (TACE) [29,30]. Aversa *et al.* reported that mTNF-α was rapidly expressed on human CD4$^+$ Th2 cells activated with Con A and that the mTNF-α-TNF-R1 interaction can provide a contact-dependent signal for the production of IgG4 and IgE [31]. In our study, we demonstrated that mTNF-*a*, which was expressed on the Th1 line 12 h after stimulation, was involved in B cell activation mediated via TNF-R2. This observation is consistent with a previous report that mTNF-α is the prime activating ligand for TNF-R2 [32]. mTNF-α is known to be involved in autoimmune disorders [33–35], but this is the first report to show the extent of mTNF-α-mediated autoimmune T-B contact help and autoantibody production. Macchia *et al.* demonstrated that HIV-infected human T cell clones did not express CD154 but did express mTNF-α, which induced polyclonal B cell activation in a contact-dependent manner [36]. This report also suggested that under certain pathological conditions mTNF-α may be up-regulated independently of CD154 expression and activate B cells. As reported previously, defective TNF function may cause autoimmunity [37]. In our preliminary experiments, the G1 line failed to

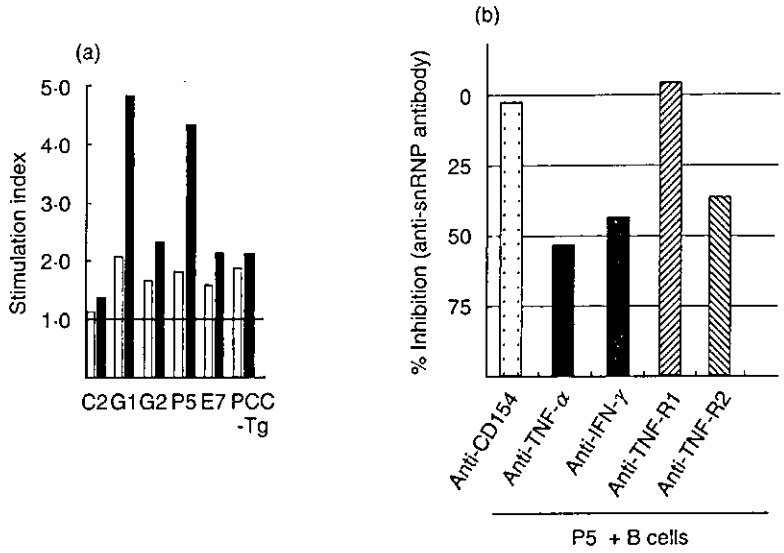

Fig. 4. *In vitro* B cell helper assay. (a) A membrane insert was used to prevent contact by the T cell line with B cells (white bar). In the absence of the membrane, G1 and P5 could induce more than the standard level of SI. Stimulation index = (concentration in culture supernatant of experimental wells)/(concentration in culture supernatant of B cells alone). The figure shows representative results of three experiments. (b) Comparison of levels of anti-snRNP antibody in the supernatant of T cell line (P5)–B cell co-culture with the blocking antibody and isotype control determined by ELISA. Anti-TNF-α, IFN-γ, and TNF-R2 MoAb inhibited anti-snRNP antibody production, while anti-TNF-R1 MoAb did not. % Inhibition = (1-{titre of anti-snRNP antibody with blocking MoAb ($O.D._{405nm}$)/anti-snRNP antibody with isotype control ($O.D._{405nm}$)}) × 100. Concentrations of blocking antibody and isotype control: 25 μg/ml. This figure shows the representative results of three experiments. □, With membrane insert; ■, without membrane insert.

induce renal diseases suggesting that mTNF-α-expressing cells may stimulate anti-snRNP antibody, but not severe organ involvement, in lupus. mTNF-α expressing recombinant virus-infected cells, however, had no effect on B cell proliferation [38], suggesting that other molecules such as CD44H or ICAM-1 [39,40] may be required for mTNF-α-mediated B cell activation.

Recently, some co-stimulatory molecules such as CD70/CD27 or CD134/CD134L have been reported to be associated with T cell-dependent B cell responses [41]. CD70 (CD27L) has also been reported to have the capacity to activate B cells through engagement with CD27 [42]. CD27–CD70 co-stimulation then contributes to enhancement of the antigen-presenting capacity of B cells or plasma cell differentiation after CD40-dependent activation [43,44]. There may also be other candidates participating in Th1-type T cell responses [45] in the absence of the CD40–CD154 system. Although our B cell activation assay with the Fab fragment derived from anti-CD27 MoAb (clone: LG.3A10) [45] was performed under the same conditions, this MoAb did not affect B cell proliferation/IgG2a secretion (data not shown). mTNF-α and CD70 therefore appear to be associated with different stages in T-cell dependent B cell activation.

How and to what extent CD154-inactive T cells are involved in autoantibody production in human SLE remains unclear. Serum levels of anti-dsDNA antibody in human lupus fluctuate with the intensity of lupus manifestations, and appear to be sensitive to the effects of immunomodulatory agents. On the other hand, it is unusual for anti-snRNP (or Sm) antibody to disappear completely [46] or show marked responsiveness to therapy. The mechanism of anti-snRNP antibody production thus appears to be different from that of anti-dsDNA antibody, and not be independent of CD154. The investigation of co-stimulatory molecules including CD154 and mTNF-α in peripheral lymphocytes from active and inactive lupus patients who have both anti-DNA and RNP antibody is a future project of ours. A recent study using (NZBxNZW)F_1 mice indicated that CD4$^+$ T lymphocytes with preformed CD154 could not provide a proliferation signal or reduce the activation threshold in B cells [47], suggesting that the direct target cells for CD154-expressing T cells may not be anti-dsDNA antibody-producing B cells. It is thus possible that the mechanisms of anti-dsDNA antibody and anti-snRNP antibody production are different in the target cells of autoantigen-reactive T cells. Our preliminary results show that autoantibodies to the whole chromatin molecule, which are thought to represent the primary immune response, could sometimes be detected in CD154-deficient MRL/*lpr* mice. Anti-dsDNA antibody production may be the secondary immune response, for which CD40–CD154 engagement is essential, while antichromatin and anti-snRNP antibody are the primary response, for which CD154 may not be essential.

CD154-deficient MRL/*lpr* mice sometimes present with a much milder renal disease but severe skin disease [21]. These results are consistent with the previous observation that the pathogenesis of skin disease induced by $\alpha\beta$ CD4$^+$ T cells may be different from that induced by $\gamma\delta$ T cells that need the CD40–CD154 signal [48]. A recent study found that the blockade of the CD40–CD154 interaction is not sufficient for complete suppression of lupus, and that additional blockade of the CD28/B7 molecule may be more beneficial [49]. Our findings also suggest that anti-CD154 MoAb therapy could suppress CD154-mediated severe lupus manifestations such as anti-dsDNA antibody synthesis and severe glomerulonephritis. Some manifestations, especially those related to the Th1-mediated immune response,

however, may be resistant to anti-CD154 MoAb treatment. We therefore suggest that it is advantageous to treat murine lupus with a combined blockade of CD154 and TNF-R2.

ACKNOWLEDGEMENTS

We thank Saeed Fatenejad for the kind gift of TNF-R2-deficient MRL/*lpr* mice and helpful comments, Jean Zhang and Ping Zhu for their technical assistance with mice management, and Tom Taylor for technical assistance with flow cytometry. This work was supported by a grant from the Donaghue Foundation (DF-96-087).

REFERENCES

1 Eisenberg RA, Tan EM, Dixon FJ. Presence of anti-Sm reactivity in autoimmune mouse strains. J Exp Med 1978; **147**:582–7.

2 Jonsson R, Tarkowski A, Backman K, Holmdahl R, Klareskog L. Sialadenitis in the MRL-l mouse: morphological and immunohistochemical characterization of resident and infiltrating cells. Immunology 1987; **60**:611–6.

3 Koh D-R, Ho A, Rahemutulla A, Fung-Leung W-P, Griesser H, Mak T-W. Murine lupus in MRL/lpr mice lacking CD4 or CD8 T cells. Eur J Immunol 1995; **25**:2558–62.

4 Peng SL, Madaio MP, Hughes DPM *et al.* Murine lupus in the antibodysence of $\alpha\beta$ T cells. J Immunol 1996; **156**:4041–9.

5 Chesnutt MS, Finck BK, Killeen N, Connolly MK, Goodman H, Wolfsy D. Enhanced lymphoproliferation and diminished autoimmunity in CD4-deficient MRL/*lpr* mice. Clin Immunol Immunopathol 1998; **87**:23–32.

6 Datta SK, Patel H, Berry D. Induction of a cationic shift in IgG anti-dsDNA autoantibodies: role of T helper cells with classical and novel phenotypes in three murine models of lupus nephritis. J Exp Med 1987; **165**:1252–68.

7 Naiki M, Chiang BL, Cawley D *et al.* Generation and characterization of cloned T helper cell lines for anti-DNA responses in NZBH-2bm12 mice. J Immunol 1992; **149**:4109–15.

8 Fatenejad S, Brooks W, Schwartz A, Craft J. Pattern of anti-small nuclear ribonucleoprotein antibodies in MRL/Mp-*lpr/lpr* mice suggests that the intact U1 snRNP particle is that autoimmunogenic target. J Immunol 1994; **152**:5523–31.

9 Peng SL, Fatenejad S, Craft J. Induction of nonpathologic, humoral autoimmunity in lupus-prone mice by a class II-restricted, transgenic $\alpha\beta$ T cell. Separation of autoantigen-specific and - nonspecific help. J Immunol 1996; **157**:5225–30.

10 Noelle RJ, Roy M, Shepherd DM, Stamenkovic I, Ledbetter JA, Aruffo A. A 39-kDa protein on activated helper T cells binds CD40 and transduces the signal for cognate activation of B cells. Proc Natl Acad Sci USA 1992; **89**:6550–4.

11 Van den Alfons JM, Noelle RJ, Roy M *et al. In vitro* CD40–gp39 interactions are essential for thymus-dependent humoral immunity. I. *In vivo* expression of CD40 ligand, cytokines, and antibody production delineates sites of cognate T–B cell interactions. J Exp Med 1993; **178**:1555–65.

12 Foy TM, Scepherd DM, Durie FH, Aruffo A, Ledbetter JA, Noelle RJ. *In vivo* CD40–gp39 interactions are essential for thymus-dependent humoral immunity. II. Prolonged suppression of the humoral immune response by an antibody to the ligand for CD40, gp39. J Exp Med 1993; **178**:1567–75.

13 Xu J, Foy TM, Lamen JD *et al.* Mice deficient for the CD40 ligand. Immunity 1994; **1**:423–34.

14 Renshow BR, Fanslow WC III, Armitage RJ *et al.* Humoral immune responses in CD40 ligand-deficient mice. J Exp Med 1994; **180**:1889–900.

15 Foy TM, Laman JD, Ledbetter JA, Aruffo A, Claassen E, Noelle RJ. gp39–CD40 interactions are essential for germinal center formation and the development of B cell memory. J Exp Med 1994; **180**:157–63.

16 Grewal IS, Xu J, Fravell R. Impairment of antigen-specific T cell priming in mice lacking CD40 ligand. Nature 1995; **378**:617.

17 Mohan C, Shi Y, Lamen JD, Datta SK. Interaction between CD40 and its ligand gp39 in the development of murine lupus nephritis. J Immunol 1995; **154**:1470–80.

18 Early GS, Zhao W, Burns CM. Anti-CD40 ligand antibody treatment prevents the development of lupus-like nephritis in a subset of New Zealand Black × New Zealand White mice. J Immunol 1996; **157**:3159–64.

19 Desai-Mehta A, Lu L, Ramsey-Goldman R, Datta SK. Hyperexpression of CD40 ligand by B and T cells in human lupus and its role in pathogenic autoantibody production. J Clin Invest 1996; **97**:2063–73.

20 Koshy M, Berger D, Crow MK. Increased expression of CD40 ligand on systemic lupus erythematosus lymphocytes. J Clin Invest 1996; **98**:826–37.

21 Ma J, Xu J, Madaio MP *et al.* Autoimmune *lpr/lpr* mice deficient in CD40 ligand. Spontaneously Ig class switching with dichotomy of antoantibody responses. J Immunol 1996; **157**:417–26.

22 Fatenejad S, Mamula M, Craft J. Role of intrastructural B and T cell determinants in the diversification of autoantibodies to ribonucleoprotein particles. Proc Natl Acad Sci USA 1993; **90**:12010–4.

23 Sheehan KCF, Pinckard JK, Arthur CD, Dehner LP, Goeddel DV, Schreiber RD. Monoclonal antibodies specific for murine p55 and p75 tumor necrosis factor receptors: identification of a novel *in vivo* role for p75. J Exp Med 1995; **181**:607–17.

24 Rubin RL. Enzyme-linked immunosorbent assay for anti-DNA and antihistone antibodies including anti-(H2A-H2B). In: Rose NR, Demacario EC, Fathey JL, Friedman H, Penn GM, eds. Manual of clinical laboratory immunology, 4th edn. Washington DC: American Society for Microbiology, 1992:735–40.

25 Jevnikar AM, Grusby MJ, Glimcher LH. Prevention of nephritis in major histocompatibility complex class II-deficient MRL-*lpr* mice. J Exp Med 1994; **179**:1137–43.

26 Chan O, Shlomchik MJ. A new role for B cells in systemic autoimmunity: B cells promote spontaneous T cell activation in MRL-*lpr/lpr* mice. J Immunol 1998; **160**:51–9.

27 Papiernik M, Pontoux C, Golstein P. Non-exclusive Fas control and age dependence of viral superantigen-induced clonal deletion in lupus-prone mice. Eur J Immunol 1995; **25**:1517–23.

28 Jacquot S, Kobata T, Iwata S, Morimoto C, Schlossman SF. CD154/CD40 and CD70/CD27 interactions have different and sequential functions in T cell-dependent B cell responses. Enhancement of plasma cell differentiation by CD27 signaling. J Immunol 1997; **159**:2652–7.

29 Black RA, Rauch CT, Kozlosky CJ *et al.* A metalloproteinase disintegrin that releases tumour-necrosis factor-α from cells. Nature 1997; **385**:729–33.

30 Moss ML, Jin S-LC, Milla ME *et al.* Cloning of a disintegrin metalloproteinase that processes precursor tumour-necrosis factor-α. Nature 1997; **385**:733–6.

31 Aversa G, Punnonen J, de Vries JE. The 26-kDa transmembrane form tumor necrosis factor α on activated CD4$^+$ T cell clones provides a co-stimulatory signal for human B cell activation. J Exp Med 1993; **177**:1575–85.

32 Grell M, Douni E, Wajant H *et al.* The transmembrane form of tumour necrosis factor is prime activating ligand of the 80 kDa tumour necrosis factor receptor. Cell 1995; **83**:793–802.

33 Kusters S, Tiegs G, Alexopoulou L *et al. In vivo* evidence for a functional role of both tumor necrosis factor (TNF) receptors and transmembrane TNF in experimental hepatitis. Eur J Immunol 1997; **27**:2870–5.

34 Akassoglou K, Probert L, Kontogeorgos G, Kollias G. Astrocyte-specific but not neuron-specific transmembrane TNF triggers inflammation and degeneration in the central nervous system of transgene mice. J Immunol 1997; **158**:438–45.

35 Georgopoulos S, Plows D, Kollias G. Transmembrane TNF is sufficient

to induce localized tissue toxicity and chronic inflammatory arthritis in transgene mice. J Inflamm 1996; **46**:86–97.

36 Macchia D, Almerigogna F, Parronchi P, Ravina A, Maggi E, Romagnani S. Membrane tumor necrosis factor-α is involved in the B cell activation induced by HIV-infected human T cells. Nature 1993; **363**:464–6.

37 Kontoyiannis D, Kollias G. Accelerated autoimmunity and lupus nephritis in NZB mice with an engineered heterozygous deficiency in tumor necrosis factor. Eur J Immunol 2000; **30**:2038–47.

38 Jumper MD, Nishioka Y, Davis LS, Lipsky PE, Meek K. Regulation of human B cell function by recombinant CD40 ligand and other TNF-related ligands. J Immunol 1995; **155**:2369–78.

39 Guo Y, Wu Y, Shinde S, Sy M-S, Aruffo A, Liu Y. Identification of a co-stimulatory molecule rapidly induced by CD40L as CD44H. J Exp Med 1996; **184**:955–61.

40 Shinde S, Wu Y, Guo Y *et al.* CD40L is important for induction of, but not response to, co-stimulatory activity. ICAM-1 as the second co-stimulatory molecule rapidly up-regulated by CD40L. J Immunol 1996; **157**:2764–8.

41 Morimoto S, Kanno Y, Tanaka Y *et al.* CD134L engagement enhances human B cell Ig production. CD154/CD40, CD70/CD27, and CD134/CD134L interactions coordinately regulate T cell-dependent B cell responses. J Immunol 2000; **164**:4097–104.

42 Kobata T, Jacquot S, Kozlowski S, Agematsu K, Schlossman SF, Morimoto C. CD27–CD70 interactions regulate B-cell activation by T cells. Proc Natl Acad Sci USA 1995; **92**:11249–53.

43 Ranheim EA, Cantwell MJ, Kipps TJ. Expression of CD27 and its ligand, CD70, on chronic lymphocytic leukemia B cells. Blood 1995; **85**:3556–65.

44 Hartwig UF, Karlsson L, Peterson PA, Webb SR. CD40 and IL-4 regulate murine CD27L expression. J Immunol 1997; **159**:6000–8.

45 Gravestein LA, Nieland JD, Kruisbeek AM, Borst J. Novel mAbs reveal potent co-stimulatory activity of murine CD27. Int Immunol 1995; **4**:551–7.

46 Fisher DE, Reeves WH, Wisniewolski R, Lahita RG, Chiorazzi N. Temporal shifts from Sm to ribonucleoprotein reactivity in systemic lupus erythematosus. Arthritis Rheum 1985; **28**:1348–55.

47 Lettesjö H, Burd GP, Mageed RA. $CD4^+$ T lymphocytes with constitutive CD40 ligand in preautoimmune (NZB × NZW) F_1 lupus-prone mice. Phenotype and possible role in autoreactivity. J Immunol 2000; **165**:4095–104.

48 Peng SL, McNiff JM, Madaio MP *et al.* $\alpha\beta$T cell regulation and CD40 ligand dependence in murine systemic autoimmunity. J Immunol 1997; **158**:2464–70.

49 Daikh DI, Finck BK, Linsley PS, Hollenbaugh D, Wofsy D. Long-term inhibition of murine lupus by brief simultaneous blockade of B7/CD28 and CD40/gp39 co-stimulation pathways. J Immunol 1997; **159**:3104–8.

How antibodies to a ubiquitous cytoplasmic enzyme may provoke joint-specific autoimmune disease

Isao Matsumoto[1,2], Mariana Maccioni*, David M. Lee[3], Madelon Maurice[4], Barry Simmons[5], Michael Brenner[3], Diane Mathis[1,2] and Christophe Benoist[1,2]

Published online: X February 2002, DOI: 10.1038/ni772

Arthritis in the K/BxN mouse model results from pathogenic immunoglobulins (Igs) that recognize the ubiquitous cytoplasmic enzyme glucose-6-phosphate isomerase (GPI). But how is joint-specific autoimmune or inflammatory disease induced by systemic self-reactivity? No unusual amounts or sequence, splice or modification variants of GPI expression were found in joints. Instead, immunohistological examination revealed the accumulation of extracellular GPI on the lining of the normal articular cavity, especially along the cartilage surface. In arthritic mice, these GPI deposits were amplified and localized with IgG and C3 complement. Similar deposits were found in human arthritic joints. We propose that GPI–anti-GPI complexes on articular surfaces initiate an inflammatory cascade *via* the alternative complement pathway, which is unchecked because the cartilage surface lacks the usual cellular inhibitors. This may constitute a generic scenario of arthritogenesis, in which extra-articular proteins coat the cartilage or joint extracellular matrix.

(AUTHOR – rephrasing in abstract OK? Note that *NI* avoids "*I*" as it introduces ambiguity and words such as "striking" as this is for the reader to decide – replaced or deleted throughout.) A hallmark of rheumatoid arthritis (RA) is the specific destruction of the synovial joints, but the role played by joint-specific autoreactivity remains controversial[1]. It is not known, for example, whether T cells are dominant players in local inflammation or whether they act upstream during the process by helping pathogenic B cells. Data obtained with the K/BxN mouse, a recently described arthritis model, have further agitated debate on these issues. These T cell receptor–transgenic (TCR-Tg) mice have a T cell repertoire that is highly skewed for a specificity directed against the major histocompatibility complex (MHC) class II A^{g7} molecule in complex with self-peptide derived from the ubiquitous glycolytic enzyme glucose-6-phosphate isomerase (GPI)[2–5]. (AUTHOR – rephrase OK?) These animals develop an aggressive form of arthritis that begins at 3–4 weeks of age. As for human RA, this spontaneous disease requires a particular MHC class II allele, is chronic, progressive, symmetrical and results in the severe destruction of cartilage and bone. A classical histological ensemble of synovitis, leukocyte invasion of the articular cavity and pannus formation causes this destruction. In this model, progression of arthritis is also typically dependent on the inflammatory cytokines interleukin 1 (IL-1) and tumor necrosis factor-α (TNF-α) (C. B. *et al.*, unpublished data). (AUTHOR – initials correct?) The articular manifestations result from arthritogenic Igs that are also directed against GPI[2,4]. High titers of these Igs develop in Tg K/BxN mice because of the preferential help that B cells expressing GPI-reactive Igs receive from the Tg T cells[6]. In the absence of lymphocytes in the host, affinity-purified anti-GPI IgG from these mice can transfer destructive arthritis and, alone, can provoke the full range of inflammatory functions that underlie the disease. Activation of the alternative pathway of complement and signaling through Fc receptors are both essential to the downstream effector phase of disease[7].

A major paradox lies in the specificity of the joint attack provoked by these Igs, which react against a ubiquitously expressed antigen. (AUTHOR – words such as "exquisite", "interesting" etc deleted throughout as per previous comment) GPI is an enzyme of the glycolytic pathway; it is essential for basic carbohydrate metabolism. Consequently, it is expressed in all cells, and GPI-deficient mouse embryos die at the two-cell stage[8]. It is normally sequestered in the cytoplasm and is only released into the circulation in minute amounts during pathological states such as liver metabolic injury or tumor growth, which correlate with cell damage or apoptosis. The presence of circulating GPI enzymatic activity in serum had been investigated as a

[1]*Section on Immunology and Immunogenetics, Joslin Diabetes Center; Department of Medicine, Brigham and Women's Hospital, Harvard Medical School, 1 Joslin Place, Boston, MA 02115, USA.* [2]*Institut de Génétique et de Biologie Moléculaire et Cellulaire (CNRS/INSERM/ULP), Strosbourg, France.* [3]*Division of Rheumatology, Immunology and Allergy, Brigham and Women's Hospital, Harvard Medical School, Boston, MA 02115, USA.* [4]*Department of Pathology, Harvard Medical School, Boston, MA 02115, USA.* [5]*Department of Orthopedic Surgery, Brigham and Women's Hospital, Harvard Medical School, Boston, MA 02115, USA.* **Present address: Depto. de Bioquímica Clínica, Universidad Nacional de Córdoba, Córdoba. 5000, Argentina. Correspondence should be addressed to C. B. and D. M. (cbdm@joslin.harvard.edu).* ***(AUTHOR – where was Maccioni when she did the work? Add number(s) pls – 1 & 2?)***

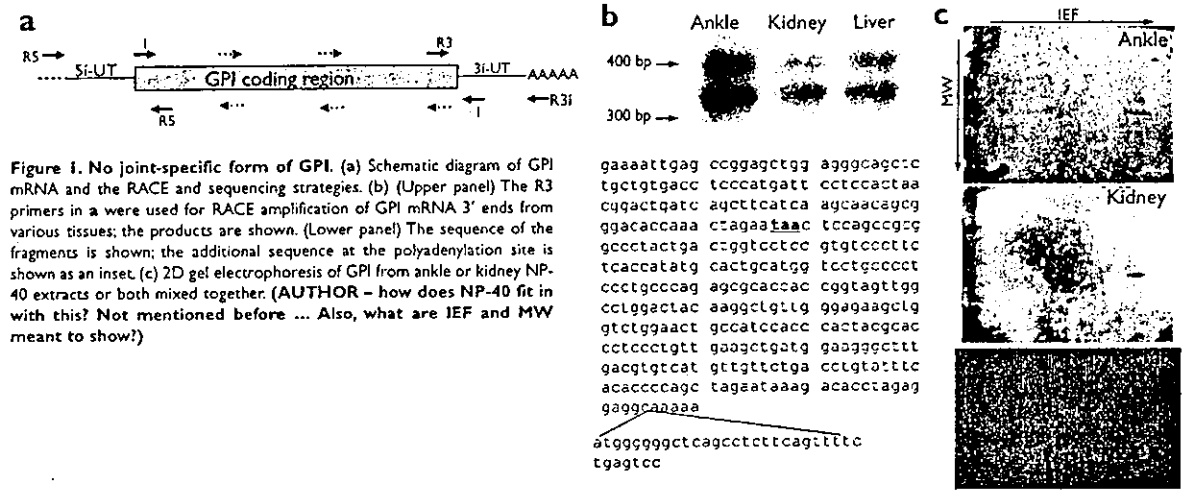

Figure 1. No joint-specific form of GPI. (a) Schematic diagram of GPI mRNA and the RACE and sequencing strategies. (b) (Upper panel) The R3 primers in a were used for RACE amplification of GPI mRNA 3′ ends from various tissues; the products are shown. (Lower panel) The sequence of the fragments is shown; the additional sequence at the polyadenylation site is shown as an inset. (c) 2D gel electrophoresis of GPI from ankle or kidney NP-40 extracts or both mixed together. **(AUTHOR – how does NP-40 fit in with this? Not mentioned before ... Also, what are IEF and MW meant to show?)**

potential diagnostic tumor marker, but was not followed up because of inconsistent results[4]. Thus, GPI makes an unlikely candidate target for arthritogenic Igs, particularly because disease manifestations in K/BxN mice appear to be limited exclusively to the joints. We explore here the potential reasons for this paradoxical joint specificity.

Results

No evident joint specificity to GPI expression

(AUTHOR – your results must be discussed in the past tense – check editing changes in line with this throughout are OK.) That the pathology provoked by anti-GPI Igs is confined to the joint raises the question of whether there might be something special about how GPI is expressed in the articulations. As a first approach, we looked for particularities in GPI gene transcripts. **(AUTHOR – what do you mean by "particularities"? This is very vague)** One possibility was that there are differences in the coding sequences of GPI mRNA in joint tissue. To address this issue, RNA was prepared from dissected ankle material and various segments of the coding region were amplified by polymerase chain reaction (PCR) using overlapping primers (**Fig. 1a**). The resulting fragments were then sequenced. Except for the known strain-specific polymorphism at amino acid position 95 (D or N)—which forms the basis for the classical genetic mapping test that relies on GPI electrophoretic polymorphism—no differences from the GenBank reference sequence for GPI mRNA were found (data not shown). Another possibility was that alternate coding region termini characterize GPI mRNA in the joint, resulting in a leader peptide and/or transmembrane region and a secreted or membrane-bound form of GPI. This possibility was tested by rapid amplification of cDNA ends (RACE) PCR[9] of both mRNA extremities (**Fig. 1a**). **(AUTHOR – by "both mRNA extremities" do you mean encoding the NH_2 and COOH termini?)** A single band was obtained by RACE at the 5′ end, which indicated a unique 5′ terminus; this was confirmed by sequencing the fragment (data not shown). At the 3′ end, two bands were detected, which showed two different transcripts were present (**Fig. 1b**). However, they proved to be irrelevant, as they were observed in equivalent proportions in RNA from joint and control tissues and merely corresponded to an alternative polyadenylation site that was of no consequence to the protein structure. **(AUTHOR – rephrase OK?)**

As a second approach, we searched for translational or post-translational modifications that could result in a different form of GPI in the joint. Extracts of various tissues were separated by two-dimensional (2D) isoelectric focusing–polyacrylamide gel electrophoresis (IEF-PAGE), and GPI was revealed by electroblotting and probing with affinity-purified anti-GPI. The mobilities of articular and extra-articular GPI were indistinguishable, as confirmed by mixing the two samples (**Fig. 1c**).

As a third approach, we compared GPI expression. Semiquantitative PCR showed that there were essentially no differences in GPI transcript levels in joint versus kidney (**Fig. 2a**). This result was confirmed by quantitative real-time PCR (**Fig. 2b**). To test whether GPI protein translation efficiency or post-translational stability varied, cytoplasmic extracts from ankle and other tissues were tested by immunoblotting

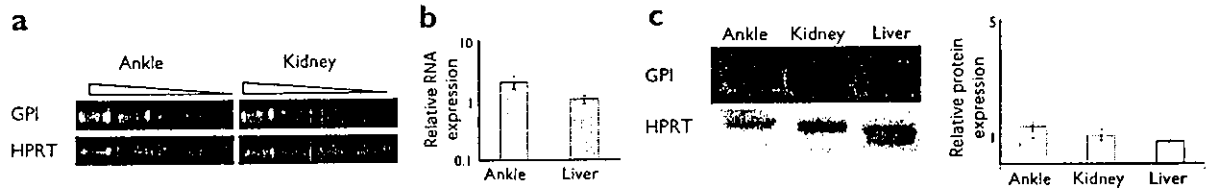

Figure 2. No overexpression of GPI in joints. (a) Semiquantitative RT-PCR analysis of GPI mRNA in RNA samples from ankle or kidney. Amplification with HPRT-specific primers was done as a control. (b) Analysis of ankle and kidney RNA by real-time quantitative PCR. (c) Expression of GPI protein analyzed by immunoblotting ankle, kidney and liver NP-40 extracts. GPI amounts, normalized on the basis of HPRT expression, are shown in the graphs. **(AUTHOR – rephrasing OK? How does NP-40 fit in?)**

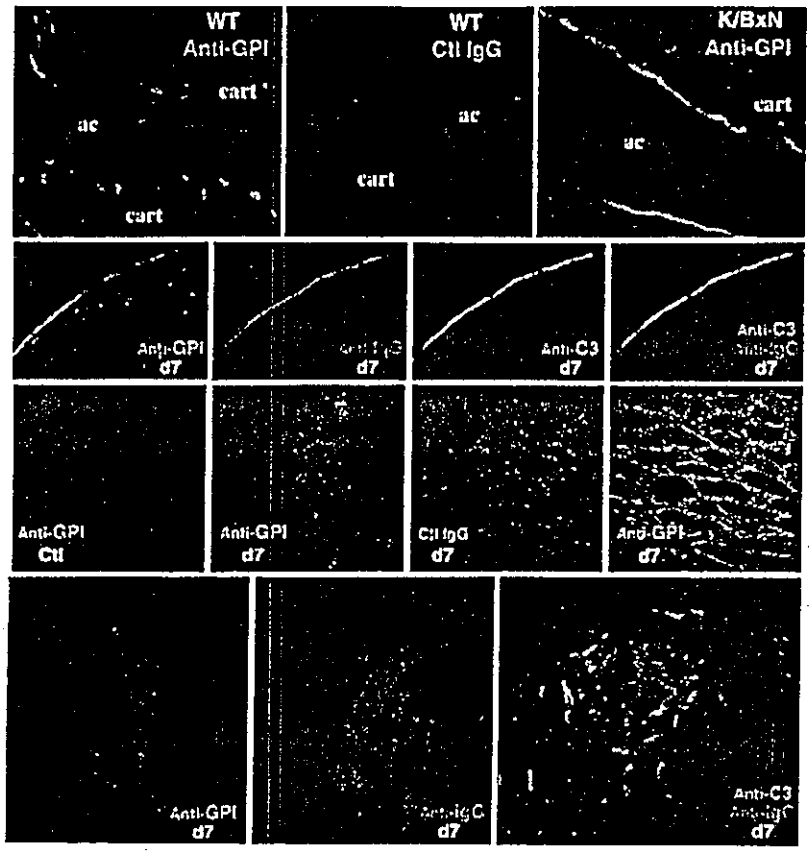

Figure 3. Presence of GPI on joint surfaces. (a,b) Serial cryostat sections from normal (WT) ankle joint stained with anti-GPI or control Ig (green); nuclei were counterstained with DAPI (blue) and examined with a confocal microscope and ×63 objective. One representative of three images are shown. Ac, articular cavity; cart, cartilage. (c) Similar staining of an ankle section from an arthritic K/BxN mouse. One representative of four images obtained from transgenic K/BxN or serum-transferred mice are shown. (d–g) Ankle cartilage surface of a B6 mouse 7 days after injection of arthritogenic K/BxN serum, stained as indicated. (g) Overlay image of e and f obtained by confocal imaging with a ×40 objective. (h,i) Kidney glomeruli from normal or K/BxN serum-injected mice stained with anti-GPI and a DAPI counterstain. One representative of three images are shown. Images were obtained by confocal imaging with a ×40 objective. (j,k) Serial muscle sections from a B6 mouse taken 7 days after injection of arthritogenic K/BxN serum. Sections were stained with anti-GPI or control Ig and a DAPI counterstain was used. Images were obtained by classical microscopy with a ×20 objective. (l–n) Kidney glomeruli from a B6 mouse taken 7 days after injection of arthritogenic K/BxN serum, stained as indicated. (l,m) Images are from the same costained section. (n) Overlay image of anti-C3 and anti-IgG stains with a DAPI counterstain. **(AUTHOR – legend was v hard to follow, repetitive text deleted and is rephrasing OK?)**

with anti-GPI (Fig. 2c). Again, when normalized relative to actin as an internal standard, no difference was observed (Fig. 2d).

Thus, we found nothing unusual about either the amounts or forms of GPI mRNA or protein in joint tissue, although a particular form of GPI produced by a minor cell population cannot be formally ruled out.

GPI deposits in the joints

As GPI expression in the joint appeared to have no unusual properties, we used immunohistology to examine its distribution in joints. Cryostat sections of several tissues from normal C57BL/6 (B6) mice were prepared without fixation or decalcification of the tissues. These sections were probed with fluorescein isothiocyanate (FITC)-conjugated anti-GPI—a polyclonal reagent prepared by affinity purification from the sera of arthritic K/BxN mice—and were examined by conventional and confocal fluorescence microscopy. As expected, GPI was homogenously distributed in the cytoplasm of all cells in all organs (data not shown). This finding was also extended to the joints: intracytoplasmic GPI was present in chondrocytes and synoviocytes and staining intensities were comparable to those of other tissues. However, there was also evidence of GPI in extracellular structures along the articular cavity; this was particularly evident at the cartilage surface, which was lined by a thin sharp crescent of GPI (Fig. 3a). No GPI was detectable within the body of the cartilage nor at the bone-cartilage junctions. Staining was specific and was not detectable with control FITC-conjugated IgG, which was prepared and used in parallel control experiments (Fig. 3b). **(AUTHOR – rephrasing in last para OK?)**

GPI deposited at the articular surface could target pathogenic Igs, which prompted the question of its fate in arthritic K/BxN Tg mice or the recipients of K/BxN serum. The amount of GPI deposited along the joint surfaces increased markedly in both types of arthritic mice (Fig. 3c). This GPI was most likely in the form of immune complexes, as deposits of IgG and C3 complement fragments were clearly visible in doubly stained serial sections (Fig. 3d–g). This localization contrasted with that observed in the joints of normal mice: in normal mice, the GPI deposits were not localized with IgG (data not shown). In arthritic mice, the GPI–anti-GPI immune complexes extended beyond the cartilage surface, along the thickened synovium and the pannus.

An explanation of joint specificity

These data suggested that pathogenic antibodies targeted GPI on the articular surface, which resulted in complex formation and complement activation. Circulating complexes of GPI–anti-GPI formed outside the joints may also have become integrated into these deposits, eventually leading to lattice formation. **(AUTHOR – rephrase of last 2 sentences OK?)** But, still, why the joint specificity? Initial analyses of K/BxN mice showed large amounts of Ig deposits in a number of tissues[2], but it was not known whether these were GPI-IgG complexes. Cryostat sections of various tissues were prepared and stained as above. The cytoplasmic GPI present in the kidney made it difficult to reliably detect GPI bound to exposed extracellular surfaces in normal mice, as had been readily detected on cartilage. However, there was a marked

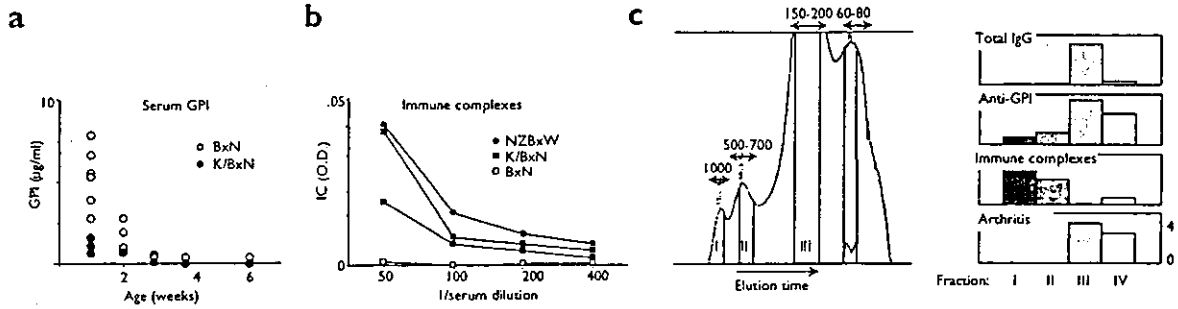

Figure 4. Circulating GPI or GPI–anti-GPI immune complexes. (a) GPI was quantified by sandwich ELISA analysis of sera from normal (B6xNOD)F_1 mice (BxN) or their arthritic Tg littermates (K/BxN). (b) Immune complexes were detected by ELISA; the target C1q was used to coat plates. Sera was taken from 5-week-old K/BxN mice, and serum from an (NZBxNZW)F_1 mouse (NZBxW) was used as a positive control for circulating immune complexes. Data are representative of two independent experiments; there were two recipient mice for each fraction. (c) K/BxN serum was fractionated by size-exclusion chromatography. (Left) Total protein elution profile; the fractions that were collected are shaded and their average molecular weights (in kD) shown. The total IgG, anti-GPI and C1q binding complex contents and arthritogenic potential of the four fractions were examined by ELISA. Data are given as arbitrary units; arthritogenic potential was assessed by injecting the fraction into naïve mice and assigning a clinical index (max clinical index determined as in [9]). **(AUTHOR – legend was hard to follow, is rephrasing OK?)**

increase in the amount of GPI could be detected in the kidney mesangium 7 days after transfer of K/BxN serum (**Fig. 3h,i**). Similarly, GPI could be detected in the muscle perimesium and/or endomesium (**Fig. 3j,k**). As in the joint, GPI localized with IgG in the kidney glomeruli (**Fig. 3l,m**), but there was a marked difference: the complement component C3 did not localize with these complexes (**Fig. 3n**). Some C3 deposits were observed, but in the peripheral membranous region of the glomeruli, and there was essentially no overlap with the mesangial GPI-IgG complexes (these C3 deposits are commonly seen in control unmanipulated mice). Thus, GPI-IgG complexes did form in extra-articular organs, but they did not initiate a complement cascade. **(AUTHOR – "This may be an important clue ..." deleted as too "chatty" for an article)**

The source of GPI and anti-GPI

Next we identified the source of the GPI deposited on the surface of articular cartilage. A sandwich ELISA was developed to assess the presence of free GPI in serum and showed circulating GPI in normal mouse serum (**Fig. 4a**). Concentrations were high in mice at 1 week of age, dropped to 400 ng/ml by 3 weeks of age and remained low thereafter. In K/BxN mice, free GPI was present in a low concentrations at week 1 and became undetectable, at least in an immunoreactive form, by week 3, which coincided with the time at which detectable anti-GPI titers initially appeared[4]. To determine whether GPI might, at that point, circulate as immune complexes, we did ELISA assays with plate-bound C1q, an indicator of immune complex formation. Complexes were indeed found in the serum of arthritic K/BxN mice at titers comparable to those found in (NZBxNZW)F_1 mice, which we used as positive controls (**Fig. 4b**). As predicted, these C1q binding complexes were only detected after 30 days of age, coincident with arthritis onset (data not shown).

Given the presence of these complexes in mice early in the onset of arthritis, we then asked whether these were the pathogenic agents, that is, whether complexes or free IgG enter the joint and cause disease. Stable immune complexes in K/BxN serum were separated from free anti-GPI IgG by high-performance gel filtration, and mice were injected with an equivalent proportion of each fraction (**Fig. 4c**). Total IgG fractionated in peak III, as expected, but ~20% of the anti-GPI was found in fractions of heavier molecular weight that contained the C1q-reactive immune complexes. Yet, when tested by injection into naïve mice, all disease-conferring activity was found in the low molecular weight fractions. This experiment must be interpreted with a degree of caution, as some complex formation will occur after transfer of free IgG (although the amount of serum GPI in an adult mouse, ~1 µg, is much smaller than the amount of anti-GPI that was injected). However, the results indicate that the immune complex fraction was not the most pathogenic fraction. **(AUTHOR – rephrasing in last para OK?)**

Applicability to human patients

A key question is whether arthritis development in K/BxN mice represents a generic mechanism that is applicable to RA or other human arthritides. In particular, is GPI also a target in humans, as has been suggested[10]? We examined, therefore, whether the pattern of GPI deposition

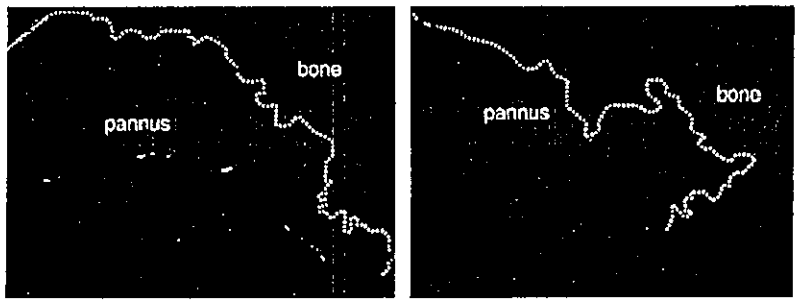

Figure 5. GPI deposits on a human RA pannus. Cryostat sections from a surgically removed digit joint of an RA patient stained with (a) anti-GPI or (b) control Ig. Conventional immunofluorescence was examined with a ×20 objective. **(AUTHOR – rephrasing OK?)**

observed in the joints of mice might be present in joints from RA patients. Two specimens of joint tissue from RA patients were prepared for immunohistological examination. In one sample, the staining intensity was modest; in the other, clear deposits of GPI were detected along the surface of the erosive pannus, although the bone surface itself was free of GPI (Fig. 5, no cartilage was present in the section). Igs were also present at the same location (data not shown); these probably corresponded to IgG deposits that have been described on the articular cavities of RA patients[11–13]. However, we did not observe the juxta-endothelial deposits described by another group[10]. Thus, patterns of anti-GPI deposits similar to those found in K/BxN mice can be observed in human RA patients. **(AUTHOR – rephrasing in last para OK?)**

Discussion

We found that GPI deposits lined the surface of the articular cavity, particularly the cartilage surface, in normal mice. As a result of these findings, we suggest a new model of arthritis pathogenesis, one that applies to disease in K/BxN mice but perhaps also to disease in humans. Diffusible extra-articular molecules bind to cartilage surfaces and serve as targets for autoantibodies, which are generated either through immune responses or loss of self-tolerance. These immobilized Igs activate the alternative complement pathway as a result of the unusual cartilage surface, which is noncellular and therefore lacks several complement inhibitors. **(AUTHOR – rephrasing in last para OK?)**

There are several tenets to this model. First, the target need not be of articular origin. None of the experiments done here identified a joint-specific form of GPI. Although it may originate in part from local release into the synovial fluid, the GPI deposited on the joint surfaces can also be passively transferred from the serum. In this respect, GPI may be only one example of several molecules that, facilitated by the absence of a basal membrane under the joint vasculature, can diffuse into the joint from the circulation. This origin may account for the arthritis found as secondary manifestations in a large variety of infections or autoimmune disorders. In these cases, immune reactions develop against self or microbial components, as occurs with hepatitis-associated arthritis, reactive arthritis that follows gut infection.

Second, the key to joint specificity may be that the development of K/BxN arthritis is dependent on activation of the alternative complement pathway[7]. With an operational mechanism parallel to that of natural killer cells, the alternative pathway can be activated on all surfaces, but is normally kept in check on self-surfaces by regulatory enzymes that destroy the spontaneously activated C3b[14]. **(AUTHOR – rephrase OK?)** These include soluble proteins (factors H and I) and cell surface proteins such as decay-accelerating factor and membrane cofactor protein. Igs bound to surfaces enhance the alternative pathway by binding C3b covalently[15,16], which protects C3b by restricting its accessibility to factor H[17]; this protection is further stabilized by properdin[18,19]. **(AUTHOR – rephrase OK?)** Cartilage is an unusual body surface. It is devoid of cell membrane–bound C3 inactivators and is only protected from alternative pathway activation by the soluble inhibitors and by the dampening effect of surface sialic acid[20,21]. Ig deposition could interfere with this process by preventing factor H access and GPI–anti-GPI complexes may also mask sialic acid residues; both these processes may contribute to turning cartilage into an activating surface. In contrast, surfaces in the kidney or muscle are more efficient at controlling the alternative pathway. Thus, the joint is a special location at which the cartilage surface maintains an uneasy alternative complement pathway equilibrium that is readily perturbed. The dominant IgG isotype in K/BxN arthritis is IgG1[7] (M. M., unpublished data), whereas IgG3 and IgG2a are the dominant isotypes for nephritis[22,23]. This is perhaps related to the fact that the classical complement pathway does play a role in kidney pathology[24]. Thus, the joint specificity of K/BxN arthritis, and perhaps more generally of arthritis in contexts of systemic immune dysregulation, may merely reflect a differential sensitivity to innate effector mechanisms rather than a response to some particular joint antigen. **(AUTHOR – rephrasing in last para OK?)**

Third, no previous link has been made between cartilage and the molecule that causes arthritis. **(AUTHOR – rephrase OK? Vague and also *NI* avoids Latin terms, as not all our readers have English as a first language)** It has been proposed that cell-surface receptors, perhaps similar to the high-affinity receptors cloned from tumor cells[25], might "present" GPI on vascular endothelial cells[10]. We have not been able to confirm endothelial surface staining on mouse sections or in the few human RA samples we analyzed. It is unlikely that cell-surface transmembrane molecules would be present on articular cartilage. We do not know which cartilage surface molecule(s) bind GPI, but hypothesize that binding may occur *via* multiple low-affinity interactions with repeated carbohydrate moieties of cartilage proteoglycans. The cartilage would then act as a low-affinity but high-avidity, "molecular sponge". That GPI is usually found as a dimer[26,27] and may be important in stabilizing such interactions. Also, it may not be mere coincidence that its natural substrates are phosphorylated sugars. It will be important to determine how GPI binds to joint surfaces and how widespread this binding may be.

Fourth, the progression of arthritis appears to entail a positive feedback loop that recruits more of the target GPI molecules and/or GPI–anti-GPI immune complexes to the surfaces of the articular cavity. The amount of GPI on the cartilage surface was far higher in arthritic transgenic or serum-transferred mice than in normal animals. In imaging experiments in which radioactively labeled anti-GPI was transferred into mice, increased binding of anti-GPI in the joint was found 48–72 h after the onset of disease, indicating that this accumulation of joint GPI is precocious **(AUTHOR – what do you mean by "precocious"?)** (U. Mahmood *et al.*, unpublished data). **(AUTHOR – unless any members of your groups are included in the "*et al*" you must fax/email us a letter of permission from this group – or delete from text)** One possibility is that early cartilage alterations, which exposed proteoglycan structures that are normally shielded, might result in increased GPI binding. It is also possible that deposited, bivalent anti-GPI would recruit more GPI to the site—as free molecules or as GPI–anti-GPI complexes—resulting in lattice formation. Consistent with this idea, analysis of the pathogenic potential of monoclonal antibodies (mAbs) has shown that arthritogenesis requires coordinate binding to multiple epitopes and the simultaneous injection of several mAbs is required for efficacy[6]. **(AUTHOR – rephrasing in last para OK?)**

Fifth, which form of anti-GPI is responsible for disease? One should distinguish between two phases. During the first phase, several arguments suggest that upon injection of GPI antibodies, free Igs enter the joint and then bind GPI onto the cavity surface, rather than immune complexes being preformed in the serum and then filtering into the cavity. **(AUTHOR – rephrase OK?)** This is because the very existence of a GPI lining along the articular cavity now provides a direct target for the binding of anti-GPI, so there is no need to invoke pre-existing immune complexes. Also, in gel filtration experiments, the pathogenic activity fractionates with free IgG not with complexes, and several attempts at enhancing the pathogenicity of mAbs or serum IgG by supplementing with titrated amounts of recombinant GPI have not worked[6]. In addition, antibodies to GPI accumulate in the joint within a matter of minutes (B.T. Wipke *et al.*[28]), which is more consistent with the immediate entry of Igs than with the accumulation of complexes. **(AUTHOR**